haematologica
Journal of The Ferrata Storti Foundation

SUMOylation inhibitor TAK-981 (subasumstat) synergizes with 5-azacitidine in preclinical models of acute myeloid leukemia

by Ludovic Gabellier, Marion De Toledo, Mehuli Chakraborty, Dana Akl, Rawan Hallal, Mays Aqrouq, Giovanni Buonocore, Clara Recasens-Zorzo, Guillaume Cartron, Abigaïl Delort, Marc Piechaczyk, Denis Tempé, and Guillaume Bossis

Received: January 6, 2023.
Accepted: August 16, 2023.

Citation: Ludovic Gabellier, Marion De Toledo, Mehuli Chakraborty, Dana Akl, Rawan Hallal, Mays Aqrouq, Giovanni Buonocore, Clara Recasens-Zorzo, Guillaume Cartron, Abigaïl Delort, Marc Piechaczyk, Denis Tempé, and Guillaume Bossis. SUMOylation inhibitor TAK-981 (subasumstat) synergizes with 5-azacitidine in preclinical models of acute myeloid leukemia. Haematologica. 2023 Aug 24. doi: 10.3324/haematol.2023.282704 [Epub ahead of print]

SUMOylation inhibitor TAK-981 (subasumstat) synergizes with 5-azacitidine in preclinical models of acute myeloid leukemia

Ludovic Gabellier[1,2,#], Marion De Toledo[1,#], Mehuli Chakraborty[1], Dana Akl[1], Rawan Hallal[1], Mays Aqrouq[1], Giovanni Buonocore[1], Clara Recasens-Zorzo[1], Guillaume Cartron[1,2], Abigaïl Delort[3], Marc Piechaczyk[1], Denis Tempé[1] and Guillaume Bossis[1]

Affiliations

1- IGMM, Univ. Montpellier, CNRS, Montpellier, France

2- Service d'Hématologie Clinique, CHU de Montpellier, 80 avenue Augustin Fliche, 34091 Montpellier, France

3- MGX, Univ. Montpellier, CNRS, INSERM, Montpellier, France

# These authors contributed equally to this work

Correspondence to marion.detoledo@igmm.cnrs.fr, denis.tempe@igmm.cnrs.fr, guillaume.bossis@igmm.cnrs.fr

Running title: TAK-981 synergizes with 5-azacitidine in AML

Disclosures: TAK-981 was obtained from Takeda Development Center Americas, Inc. Guillaume Cartron is consultant for Roche and BMS-Celgene, member of the advisory boards of MabQi, Ownards Therapeutics, MedXcell and receive honoraria from Abbvie, Sanofi, Gilead, Janssen, Roche, BMS-Celgene, Takeda Pharmaceuticals. The remaining authors declare no financial competing interests.

Acknowledgments

We thank the members of the "Ubiquitin Family in Hematological Malignancies" group, Takeda Development Center Americas (Lexington, MA), for providing TAK-981 and Dr Allison Berger for critically reading the manuscript.

Fundigs

Funding was provided by the CNRS, the Ligue Nationale contre le Cancer (DA, MC, MP), the Fondation pour la Recherche Médicale (contract FDM201906008566, LG), INCa_16072, the Fédération Leucémie Espoir, the Association Laurette Fugain, the Fondation ARC pour la recherche sur le cancer and the Agence Nationale pour la Recherche ("Investissements d'avenir" program; ANR-16-IDEX-0006; project SUMOLAM). The HEMODIAG_2020 collection was funded by the Montpellier University Hospital, the Montpellier SIRIC and the Languedoc-Roussillon Region. MGX acknowledges financial support from the France Génomique National infrastructure, funded as part of "Investissements d'Avenir" program managed by the Agence Nationale pour la Recherche (contract ANR-10-INBS-09).

Data availability

The RNA-Seq sequencing data are available on Gene Expression Omnibus with accession number GSE212330. All other data are available in the main text or the supplementary materials.

Authors contributions

LG designed and performed the experiments on cell lines, patient cells and mouse models. MdT conceived and performed in vivo experiments. MC prepared samples for RNA-Seq and performed qPCR. DA, MA, GiB analyzed viability and differentiation of AML cell lines. RH

participated to PBMC and NK purifications. MA, RH and DA performed validation qPCR. AD prepared RNA-Seq libraries and sequenced them. CRZ performed microbead-based assay. GC provided patient samples. DT conceived and analyzed RNA-Seq experiments and performed GSEA analysis. MP provided funding for the study. GB supervised the study and provided fundings. LG, MdT, DT, MP and GB wrote the manuscript.

Abstract

Acute Myeloid Leukemias (AML) are severe hematomalignancies with dismal prognosis. The post-translational modification SUMOylation plays key roles in leukemogenesis and AML response to therapies. Here, we show that TAK-981 (subasumstat), a first-in-class SUMOylation inhibitor, is endowed with potent anti-leukemic activity in various preclinical models of AML. TAK-981 targets AML cell lines and patient blast cells *in vitro* and *in vivo* in xenografted mice with minimal toxicity on normal hematopoietic cells. Moreover, it synergizes with 5-azacitidine (AZA), a DNA-hypomethylating agent now used in combination with the BCL-2 inhibitor venetoclax to treat AML patients unfit for standard chemotherapies. Interestingly, TAK-981+AZA combination shows higher anti-leukemic activity than AZA+venetoclax combination both *in vitro* and *in vivo*, at least in the models tested. Mechanistically, TAK-981 potentiates the transcriptional reprogramming induced by AZA, promoting apoptosis, alteration of the cell cycle and differentiation of the leukemic cells. In addition, TAK-981+AZA treatment induces many genes linked to inflammation and immune response pathways. In particular, this leads to the secretion of type I interferon (IFN-I) by AML cells. Finally, TAK-981+AZA induces the expression of Natural Killer (NK)-activating ligands (MICA/B) and adhesion proteins (ICAM-1) at the surface of AML cells. Consistently, TAK-981+AZA-treated AML cells activate NKs and increase their cytotoxic activity. Targeting SUMOylation with TAK-981 may thus be a promising strategy to both sensitize AML cells to AZA and reduce their immune-escape capacities.

Introduction

Acute Myeloid Leukemias (AML) are severe hematologic malignancies resulting from the acquisition of oncogenic mutations by hematopoietic stem or progenitor cells. AML cells, which are blocked at intermediate stages of differentiation, proliferate and infiltrate the bone marrow, thereby disrupting normal hematopoiesis[1]. Fit patients are usually treated with intensive chemotherapy based on the combination of an anthracycline (daunorubicin-DNR or idarubicin) and the nucleoside analogue, cytarabine (Ara-C). Relapses are however frequent and overall survival (OS) remains very poor. In the past few years, various new molecules improving AML prognosis have been approved. In most cases, they target mutated oncogenes such as IDH1/2 or FLT3, which restricts their use to patients carrying these mutations[2]. Unfit patients who cannot receive chemotherapy because of age or comorbidities are generally treated with hypomethylating agents, in particular 5-azacitidine (AZA)[3]. In cells, this cytidine analog is metabolized into 5-aza-dCTP and incorporated into DNA during replication, where it can form covalent adducts with DNA-methyl transferases (DNMT). This triggers ubiquitin-proteasome-dependent depletion of DNMTs[4] and results in a progressive loss of DNA methylation at CpG dinucleotide motifs. The prevalent model to explain the therapeutic effect of AZA is that reduced methylation of CpGs leads to the reactivation of silenced tumor suppressor genes as well as genes involved in differentiation, which are generally hypermethylated at cis-regulatory regions in cancer cells[5]. The clinical benefit of AZA treatment is however limited with a 4 to 5-month increased OS compared to other AML therapies[6]. Its combination with the BCL2 inhibitor venetoclax (VEN) significantly improves patient response and OS[7,8]. This combo is now used as first-line therapy for patients unfit for standard chemotherapies. Nevertheless, a proportion of AML patients respond poorly to this regimen or acquire resistance[9,10].

SUMO proteins are peptide post-translational modifiers with structural homology to ubiquitin. Whilst human genome encodes for 5 SUMO genes (SUMO-1 to -5), the main conjugated isoforms are SUMO-1, -2 and -3, the latter two being almost identical[11]. SUMOylation involves a SUMO-activating E1 enzyme (UBA2/SAE1), a SUMO-conjugating E2 enzyme (UBC9) and several E3 factors. SUMOylation is highly dynamic thanks to various isopeptidases, which can release SUMO from conjugated targets. SUMOs are conjugated to lysines of thousands of proteins (>6000 identified in cancer cells[12], around 1000 in healthy mouse tissues[13]) to modify their function and fate[14]. As such, SUMOylation has been implicated in the regulation of most cellular functions[11]. One of its best-characterized roles concerns the regulation of gene expression[15,16]. We have previously shown that SUMOylation limits the anti-leukemic activity of both chemotherapies (DNR and Ara-C)[17] and differentiation therapies[18] in AML. This suggested that targeting the SUMO pathway could improve AML responses to therapies. A recent breakthrough in the field of SUMOylation is the discovery of TAK-981 (subasumstat), a first-in-class SUMO E1 inhibitor with very high potency and specificity[19]. TAK-981 has potent anti-tumoral activity in syngenic mouse models grafted with murine lymphoma or pancreatic tumor cells through the induction of a strong type-1 interferon (IFN-I)-dependent anti-tumor immune response[20,21]. Indeed, TAK-981 activates dendritic cells, cytotoxic $CD8^+$ T-cells, memory B cells, Natural Killer (NK) and macrophages[20–24]. Moreover, TAK-981 increases antigen presentation by cancer cells, further enhancing anti-tumor immune response[22]. In addition to these effects on the immune micro-environment, TAK-981 can directly induce cancer cells death[21,25–27]. However, the relative contribution of the direct and indirect anti-tumoral activities of TAK-981 remains to be clarified.

Here, we have addressed the therapeutic potential of TAK-981 in AML. We found that TAK-981 has potent anti-leukemic activity, in particular when combined with AZA. TAK-981 exacerbates the transcriptional reprogramming induced by AZA. In addition to genes involved in differentiation and apoptosis, TAK-981+AZA induces inflammation- and immune response-related transcriptional programs. In particular, AML cells exposed to TAK-981+AZA show increased secretion of IFN-I. Finally, they express, at their membrane, NK adhesion molecules (ICAM-1) and ligands of NK activating receptors (MICA/B), leading to an enhanced NK-mediated cytotoxicity towards AML cells. Altogether, our data suggest that combining the inhibition of SUMOylation by TAK-981 and DNA methylation by AZA could be a promising strategy for AML treatment.

Methods

Bioluminescent cell line generation, patient cell cultures, flow cytometry and RNA-Seq analysis are described in supplemental methods.

Pharmacological inhibitors and reagents

TAK-981 was obtained from Takeda Development Center Americas, Inc. Azacytidine (5-azacytidine - AZA) was from StemCell and resuspended in RPMI prior to each experiment. Daunorubicin hydroxychloride (DNR) and aracytine (aracytosine-β-D-arabinofuranoside-ARAC) were from Sigma-Aldrich, venetoclax (VEN) from MedChemExpress. All antibodies used are described in Supplementary Table 1.

Cell Lines and Culture Conditions

Human AML cell lines (U937, THP-1, HL-60, MOLM14, MV4.11) were obtained by the American Type Culture Collection and regularly tested for *Mycoplasma* contamination. They

were cultured as previously described[28] at 37°C in the presence of 5% CO_2 in RPMI 1640 medium supplemented with 10% heat-decomplemented fetal bovine serum (FBS), penicillin and streptomycin. Cells were seeded at 0.3 x 10^6/mL one day before being drug-treated.

Patient and healthy donor samples

Bone marrow aspirates and blood samples were collected after obtaining written informed consent from patients or donors under the frame of the Declaration of Helsinki and after approval by the Institutional Review Board (Ethical Committee "Sud Méditerranée 1," ref 2013-A00260-45, HemoDiag collection). Healthy donor leukocytes were collected from blood donors of the Montpellier Etablissement Français du Sang. Fresh leukocytes were purified by density-based centrifugation using Histopaque 1077 (Sigma-Aldrich). NK cells were purified using EasySep Human NK Cell Isolation kit (StemCell Technologies).

AML mouse xenograft model

All experiments on animals were approved by the Ethics Committee of the Languedoc-Roussillon (2018043021198029 #14905 v3). For Cell Line Derived Xenograft (CLDX) and Patient Derived Xenograft (PDX) experiments, female NOD/LtSz-SCID/IL-2Rychain null (NSG) mice (Charles River) mice (6-10 weeks old) were treated using respectively 20 mg/kg and 30mg/kg busulfan IV injections (SIGMA B2635, France) 48 hours before cell engraftment. 1x10^6 cells (cell lines) or 1.5x10^6 cells (patient's cells) were injected in the tail vein.

Assessment of NK cytotoxicity towards AML cells

Target cells (THP-1-LucZsGreen) were cocultured at a 1:1 ratio in 96-well plates with primary NK cells purified from fresh PBMCs of healthy donors. Real-time fluorescence was assessed for 15 hours using the IncuCyte S3 Live Cell imaging system (Sartorius) in the non-adherent cell-by-cell mode, using a 20X objective, 4 images/well and 1 image/hour. Analyses were

performed by measuring the relative integrated green fluorescence intensity using IncuCyte 2021C software.

Statistical analyses

Statistical analyses of the differences between data sets were performed using one-way ANOVA for normal distribution data and Kruskal-Wallis or Friedman tests for non-Gaussian distribution data (GraphPad Prism, GraphPad v9.4.0). Overall mouse survivals were estimated for each treatment group using the Kaplan-Meier method and compared with the log-rank test. P-values of less than 0.05 were considered significant (*, $P < 0.05$; **, $P < 0.01$; and ***, $P < 0.001$, ns = not significant).

Results

TAK-981 synergizes with AZA to induce AML cell death *in vitro*

To characterize the effect of the SUMOylation inhibitor TAK-981 on AML cells, we first monitored its impact on SUMOylation in 3 model AML cell lines, HL-60, U937 and THP-1. After 24 hours, TAK-981 induced a strong decrease in global SUMOylation by SUMO-1 and SUMO-2/3 at 10 nM and an almost complete loss at 100 nM (Figure 1A and Supplementary Figure 1A). Although the extent of deSUMOylation was similar between the 3 cell lines, U937 and THP-1 cells were highly sensitive to TAK-981, whilst HL-60 were unaffected after 24 hours of treatment (Figure 1B). Importantly, TAK-981 did not significantly affect the viability of normal mononuclear cells derived from either bone marrow (BMDMC) or peripheral blood (PBMC) under the same conditions (Figure 1C). Then, to determine whether SUMOylation inhibition could synergize with the drugs most commonly used for AML treatment, we combined TAK-981 with either DNR, ARA-C or AZA to treat HL-60, the least

sensitive cell line to TAK-981, for 24 hours (Figure 1D and Supplementary Figure 1C). TAK-981 synergized with all 3 drugs, the strongest synergy being with AZA (Figures 1D).

As several rounds of replication are necessary to obtain maximal AZA-induced hypomethylation, we performed viability assays after 72 hours of treatment. Under these conditions, all cell lines showed sensitivity to TAK-981 alone, HL-60 and U937 being however less sensitive than THP-1 cells (Supplementary Figure 1B). A synergistic cytotoxicity was seen between TAK-981 and AZA for these 3 cell lines (Figures 1E and Supplementary Figure 1D). TAK-981 and AZA combination was also more efficient than the single treatments on MOLM14 and MV4.11 cell lines (Supplementary Figure 1E). For all cell lines, AZA+TAK-981 combination was more efficient than AZA+VEN combination at decreasing AML cell line viability *in vitro* (note the differences in VEN and TAK-981 doses used, Supplementary Figure 1E). We then treated primary AML cells from 17 different patients. Both AZA and TAK-981 treatment led to a significant reduction in the number of leukemic cells, but the most important effect was obtained with the combination of the two drugs, with however some variability between patient samples (Figure 1F and Supplementary Table 2). This variability might be related to the cytogenetic characteristics of the patients, as those with abnormal karyotypes were more sensitive to TAK-981+AZA than those with a normal karyotype (Supplementary Figure 2A). In addition, patients from the more differentiated M4/M5 subgroups of French American British (FAB) classification were more sensitive to TAK-981 than those from the more immature M1/M2 subgroups (Supplementary Figure 2B). Finally, treatments had no significant effects on BMMC from healthy donors cultured under the same conditions, although TAK-981, when used alone, tend to slightly increase their numbers (Figure 1G). Altogether, these data suggest that inhibition of SUMOylation with

TAK-981 affects the viability of AML cells and synergizes *in vitro* with the hypomethylating agent AZA.

TAK-981+AZA combo has anti-leukemic activity in preclinical AML models

To further delineate the therapeutical potential of the TAK-981+AZA combination, we performed *in vivo* experiments using NOD-SCID-gammaIL2R^{null} (NSG) mice. First, to ensure the efficiency of TAK-981 *in vivo*, we used a microbead-based assay[29,30] to monitor its ability to inhibit SUMOylation activity. TAK-981 treatment leads to a 70% decrease in SUMOylation activity in the bone marrow of NSG mice after 5 hrs and a progressive recovery to basal levels after 24 hrs (Supplementary Figure 3A). Second, NSG mice were grafted intravenously with bioluminescent THP-1 (Supplementary Figure 3B) or U937 cells (Supplementary Figure 4A). TAK-981 and AZA monotherapies limited tumor progression (Figures 2A, Supplementary Figures 3C and Supplementary Figure 4B-C) and significantly extended mice survival (Figure 2B and Supplementary Figure 4D) for both THP-1 and U937. TAK-981+AZA combination had a much higher anti-leukemic effect than the monotherapies (Figures 2A-B and Supplementary Figures 4B-D). Finally, it was also more efficient than VEN+AZA combination at both limiting THP-1 cells proliferation *in vivo* and extending mice survival (Figures 2C-D and Supplementary Figure 3D).

We then turned to Patient-Derived Xenografts (PDX) (Supplementary Table 2). Once engrafted patient cells became detectable in blood, mice were treated with one cycle of TAK-981 and/or AZA and the number of leukemic cells was analyzed in spleen and bone marrow. For the first patient tested (PDX #1), TAK-981 decreased tumor burden on its own in the spleen. TAK-981+AZA treatment was more efficient than TAK-981 alone at decreasing

tumor burden in both spleen and bone marrow (Figure 2E). Similar results were obtained with two other PDX (PDX #2 and PDX #3)(Figures 2F and Supplementary Figure 4E). AZA was highly efficient on its own on one of them (PDX #3), thus limiting the benefit of its combination with TAK-981 in this case (Supplementary Figure 4E). Altogether, these data show in preclinical models that targeting SUMOylation with TAK-981 can exert an anti-leukemic effect *in vivo*, which is increased when combined with AZA.

TAK-981 amplifies AZA-induced transcriptional reprogramming and favors apoptosis

To study the molecular mechanisms underlying the synergy between TAK-981 and AZA in AML, we performed RNA-Seq experiments in U937 cells treated for 72 hours. TAK-981 showed limited effects on gene expression with 112 genes up-regulated and 3 genes down-regulated more than 2-fold (Figure 3A). AZA induced a much broader transcriptional reprogramming with 1684 genes up- and 225 genes down-regulated (Figure 3B). The highest impact on transcription occurred with the TAK-981+AZA combo, with 2947 genes up-regulated and 850 genes down-regulated more than 2-fold (Figure 3C and Supplementary Table 3). Most genes up- or down-regulated upon AZA (orange and purple dots, respectively) had higher fold changes upon TAK-981+AZA combination (Figure 3D). This suggests that inhibition of SUMOylation with TAK-981 amplifies AZA-induced modulation of gene expression. Accordingly, Gene Set Enrichment Analysis (GSEA) revealed that most gene signatures enriched in AZA treated cells have higher normalized enrichment scores (NES) upon TAK-981+AZA treatment (Figure 3E). The most enriched pathways in the TAK-981+AZA versus mock- (Figure 3E), AZA- (Supplementary Figure 5A) and TAK-981- (Supplementary Figure 5B) treated cells, are linked to cell death as well as inflammation and immune system

(see below). To avoid measuring transcriptional effects indirectly linked to the induction of cell death, we performed the RNA-Seq analysis in U937 treated with doses of AZA and TAK-981 (10 nM each) suboptimal to induce apoptosis (Figure 4A). However, in line with the activation of transcriptional programs related to cell death, combinations of AZA and TAK-981 at higher doses led to a massive apoptosis both in U937 and THP-1 cells (Figure 4A). For both cell lines, TAK-981+AZA was more efficient than VEN+AZA at inducing apoptosis (Figure 4A). Finally, the most down-regulated gene signatures in TAK-981+AZA treated cells are related to cell cycle progression, in particular MYC and E2F target genes (Figure 3E and Supplementary Figure 3A-B). We confirmed that *c-MYC* itself is down-regulated upon TAK-981+AZA treatment in U937 cells (Supplementary Figure 5C). In the THP-1 and HL-60 cell line, we did not observe a significant modulation of *c-MYC* but TAK-981+AZA induced a strong up-regulation of *CDKN1a*, which encodes the $p21^{(WAF1/CIP1)}$ cell cycle inhibitor and is known to be repressed by c-MYC[31], suggesting a downregulation of the MYC pathway in these cell lines as well (Supplementary Figure 5D). TAK-981, in particular when combined with AZA, altered cell cycle progression with decreased percentage of cells in G1 (Figure 4B). Altogether, this suggests that the amplification of AZA-induced transcriptional reprogramming by TAK-981 leads to decreased proliferation and increased apoptosis of the leukemic cells, providing an explanation for the synergy between the two drugs.

TAK-981+AZA favors AML cells differentiation

Restoration of differentiation participates to the anti-leukemic action of various drugs, including hypomethylating agents[32]. Gene signatures related to myeloid differentiation were enriched in TAK-981+AZA compared to mock, AZA and TAK-981 treatments (Figure 5A and

Supplementary Table 4). We confirmed by qRT-PCR that TAK-981+AZA combo leads to a stronger increase in the expression of the myeloid marker CD14 compared to the single treatments in U937 cells (Figure 5B). TAK-981+AZA also induced CD14 expression at the surface of U937 xenografted in mice (Figure 5C). Similarly, CD14 expression was found induced in THP-1 cells, with again a maximal effect obtained for the TAK-981+AZA combination (Figure 5D). As a comparison, VEN+AZA combination also induced CD14 expression in THP-1 cells at however lower levels (Supplementary Figure 6). Finally, the pro-differentiation effect of TAK-981+AZA treatment was confirmed on patient cells *in vivo*, both in the blood (Figure 5E) and bone marrow (Figure 5F) of PDX mice (PDX #1), with increased expression of CD14 and CD15 at the surface of the leukemic cells. Altogether, our data suggest that the anti-leukemic action of the combination of TAK-981 and AZA is associated to the reactivation of leukemic cells differentiation.

TAK-981+AZA induces the secretion of IFN-I by AML cells

As mentioned above, inhibition of SUMOylation increases AZA-induced expression of genes linked to inflammatory response and immunity (Figure 3E). In particular, this concerns IFN-I response pathway (Figure 6A), with genes such as Interferon Regulatory Factors (IRFs) being maximally up-regulated upon TAK-981+AZA in both U937 (Figure 6B) and THP-1 cells (Figure 6C-D). Accordingly, TAK-981+AZA induced the production of IFN-α by THP1-cells (Figure 6E). We then analyzed IFN-α production *in vivo* by intracellular labelling of IFN-I on AML patient cells recovered from the bone marrow of PDX mice (PDX #1). Only TAK-981+AZA induced an increase in IFN-α production by the AML cells (Figure 6F).

Thus, in addition to a direct effect on AML cells differentiation, proliferation and viability, TAK-981+AZA combination enhances the secretion of IFN-I by AML cells, which may stimulate innate and/or adaptative anti-tumor immune response.

TAK-981 induces the expression of NK cells ligands on AML cells and activates NK cytotoxicity

NK cells play critical roles in cancer immune surveillance, including in AML[33]. Within the gene signatures linked to immune response enriched in TAK-981+AZA versus mock-, AZA- or TAK-981-treated U937 cells, we identified several related to the activation of NK cells (Figure 7A and Supplementary Table 4). Among the genes of this signature, we focused on the adhesion molecule ICAM-1, which is required for target cells to bind to NK through its interaction with LFA-1[34], as well as on the MICA/B ligands of the NK-activating receptor NKG2D present on NK cells[35]. TAK-981 increased the expression of ICAM-1 and MICA/B at the surface of THP-1 cells, which was further increased by addition of AZA (Figures 7B-C). *In vivo*, ICAM-1 expression at the surface of xenografted patient cells was also increased by both TAK-981 and TAK-981+AZA treatments (Figure 7D) whereas, only TAK-981+AZA led to an increased MICA/B expression (Figure 7E). To assess whether these treatments could enhance the activation of NK cells, we co-cultured PBMCs purified from the blood of 6 different healthy donors as a source of NK cells together with THP-1 cells, previously treated with TAK-981, AZA or the drugs combination. The expression of the activation marker CD69 was increased at the surface of NK cells when they were co-cultured with TAK-981- or TAK-981+AZA-treated THP-1 compared to mock- or AZA-treated cells (Figure 7F). Finally, we monitored the cytotoxicity of purified NK cells isolated from 5 healthy donors towards THP-1 cells using live

cell imaging. NK cytotoxicity was higher on THP-1 cells that had been previously treated with TAK-981+/-AZA compared to mock- or AZA-treated cells (Figures 7G-H). Altogether, our data suggest that TAK-981+AZA favors the recognition and lysis of AML cells by NK cells, which could contribute to the anti-leukemic activity of this treatment.

Discussion

Here, we report that the SUMOylation inhibitor TAK-981 has anti-leukemic activity in various AML preclinical models. Moreover, it synergizes with AZA, a DNA hypomethylating agent widely used for AML treatment. TAK-981 and AZA combo induces a broad transcriptional reprogramming of AML cells underlying pleiotropic effects. These include increased apoptosis, alteration of the cell cycle, differentiation of the leukemic cells, induction of IFN-I secretion and enhanced expression of NK cells ligands at the surface of AML cells, which stimulates NK cytotoxicity towards them (Figure 8).

Accumulating evidence suggest that alteration in SUMOylation can both contribute to tumorigenesis and affect response to therapies in various cancers[36]. This is notably the case for AML[37]. Different inhibitors of SUMOylation such as anacardic acid[17], 2D-08[18,38] and McM025044[39] showed *in vitro* toxicity for leukemic cell. However, their low activity (µM range) and poor pharmacological properties prevented further preclinical studies. The discovery of TAK-981 now allows to envision SUMOylation inhibition in cancer patients. Five phase I/II clinical trials are ongoing in solid tumors (NCT03648372, NCT04381650), multiple myelomas (NCT04776018) and lymphomas (NCT03648372, NCT04074330). Our data obtained in preclinical models of AML provide a rationale for evaluating TAK-981 in AML treatment. Importantly, we observed minimal toxicity of TAK-981 on normal blood and bone marrow mononuclear cells (Figure 1C, 1G) or when administered to mice (Figure 2).

Although TAK-981 can kill leukemic cells *in vitro* and *in vivo*, its antitumor activity is relatively limited when used as monotherapy. However, its combination with AZA has a largely superior anti-leukemic activity. Combination therapies are increasingly considered to achieve stronger responses to cancer treatments and to limit relapses, including in AML[40]. This notably concerns AZA, whose combination with various drugs, in particular VEN, has improved clinical responses[3]. Nevertheless, many patients are refractory to VEN+AZA regimen or relapse after treatment[9,10]. This is for example the case of patients suffering from monocytic AML (FAB M4 and M5)[41]. It is therefore interesting that TAK-981+AZA shows more efficiency than VEN+AZA for all cell lines tested. In particular, TAK-981+AZA was more efficient than VEN+AZA at inducing apoptosis, cell cycle defects and differentiation of the monocytic cell lines U937 and THP-1. In addition, in our *in vitro* experiments on patient cells (Figure 1F and Supplementary Figure 2B), AML cells from the more differentiated M4 and M5 subgroups were as sensitive (even slightly more sensitive) to TAK-981+AZA treatment than less differentiated AML cells from the M1 and M2 subgroups. Patients who are refractory to VEN+AZA regimen might therefore be sensitive to TAK-981+AZA treatment.

The synergy between AZA and TAK-981 likely resides in the ability of TAK-981 to enhance the action of AZA on transcription. A large number of transcription factors, co-activators and co-repressor complexes, the basal transcription machinery and histones are SUMOylated[15,16,42]. In general, SUMOylation of protein-complexes rather than individual proteins within these complexes mediates the biological effects of SUMOylation, which include the stabilization of these complexes[43] or the recruitment of SUMO Interacting Motif- (SIM) containing proteins[44,45]. For example, SUMOylation of chromatin bound proteins can favor the recruitment of co-repressor complexes such as those containing Histone Deacetylases (HDAC)[46–48] or the Histone Methyl Transferase SETDB1[49] via SUMO-SIM interactions. We

show that inhibition of SUMOylation *per se* has limited effects on gene expression. Although surprising considering the high number of SUMOylated proteins present on gene regulatory regions, SUMOylation is thus dispensable for gene expression in basal conditions. However, inhibition of SUMOylation largely increases the expression of most AZA-induced genes. Hence, it is likely that the effect of TAK-981 on AZA-induced transcriptional reprogramming is due to the global deSUMOylation of proteins bound to gene regulatory regions rather than the consequence of the deSUMOylation of specific proteins present in these regions. This deSUMOylation would create a permissive environment for transcription, likely by affecting the recruitment and activity of transcription regulating- and/or chromatin remodeling-complexes. This would therefore amplify the transcriptional regulation of genes, whose cis-regulatory regions have been hypo-methylated by AZA. Of note, we have recently shown that inhibition of SUMOylation limits the transcriptional reprogramming induced by DNR in AML cells after few hours of treatment[50]. This suggests that inhibitors of SUMOylation could have different global impact on gene expression depending on the duration of the treatment (hours versus days) and/or the drugs they are associated with.

We also do not exclude that other mechanisms than transcriptional reprogramming might be at play to explain the synergy between AZA and TAK-981. Poly-SUMOylation of DNMT1 was shown to be triggered by decitabine, another hypomethylating agent, which induces crosslink between DNMT1 and DNA. This leads to its RNF4 mediated ubiquitylation and promotes the resolution of the DNA-protein crosslinks (DPCs)[4,51]. Accordingly, inhibition of SUMOylation increases decitabine-induced-DPCs, ultimately resulting in DNA damage and cell death in models of lymphoma[52]. However, these studies were performed with high doses (1-10 µM) of decitabine, which is much more prone to induce DPC and DNA damage than AZA at the same doses[53]. In the condition used in our transcriptomic study (10 nM of

AZA for 72 hours), it is unlikely that AZA induces massive DPCs and subsequent DNA damage. Moreover, the transcriptional reprogramming we characterized in AML was observed at sublethal doses of the drugs, further supporting the idea that it did not involve DPC-induced DNA damages.

Our data point to pleiotropic effects of the TAK-981+AZA combo to eliminate AML cells through increased apoptosis, decreased proliferation and induction of myeloid differentiation. The contribution of these different pathways to the anti-leukemic activity of the TAK-981+AZA combo differs depending on the concentrations of the drugs. At the highest doses, apoptosis is likely central to the anti-leukemic action of TAK-981+AZA. At lower doses, differentiation might be the main contributor to the decreased cell proliferation upon TAK-981+AZA treatment. Indeed, induction of differentiation is critical for the action of various AML therapies, including All Trans Retinoic Acid (ATRA) and arsenic trioxide in Acute Promyelocytic Leukemia (APL) subtype of AML[54] as well as IDH1 and FLT3 inhibitors[55].

In addition to the direct effect on AML cells proliferation and survival, TAK-981+AZA combination induces many genes linked to inflammation and immunity. This is notably the case for the IFN-I pathway, which has been reported to be activated by both AZA in cancer cells[56,57] and by TAK-981 in immune cells[20,21]. IFN-I induction can then induce an anti-tumor immune responses in these models[20,21,23]. Although TAK-981 on its own weakly induced IFN-I pathway, its combination with AZA largely increased IFN-I secretion by AML cells themselves. Although systemic IFN-I based therapies have proven disappointing in terms of clinical efficacy with important toxicities[58], controlled and localized secretion of IFN-I by AML cells might be sufficient to elicit an anti-leukemic immune response devoid of toxicity.

Finally, our work suggests an important role for NK cells in the elimination of TAK-981-treated AML cells. NKs can eliminate tumor cells directly by inducing their lysis or indirectly through the secretion of cytokines such as IFN-γ or TNF-α. AML patients survival is highly correlated with the number and activity of NK cells[35]. However, NKs are often poorly functional in these patients. In particular, NKs from AML patients are often defective in the expression of activating receptors (DNAM1, NKp30, NKp46) or overexpress inhibitory KIR receptors. Finally, AML cells develop immunosuppressive strategies to escape NK-mediated cell lysis, such as down-regulation or shedding from their cell surface of ligands of the NK-activating receptor NKG2D (MICA/MICB and ULBP1-6)[35]. It was therefore interesting to observe that TAK-981+AZA treatment leads to up-regulation of MICA/MICB at the surface of AML cells. In addition, we also detected an up-regulation of adhesion molecule ICAM-1, whose binding to the LFA-1 receptor on NK is required for efficient lysis of AML cells[34]. The combined secretion of cytokines and expression of NK-activating markers by AML cells could explain the increased activation and enhanced cytotoxicity of NKs towards TAK-981+AZA treated AML cells.

In conclusion, our work suggests that targeting SUMOylation with TAK-981 may be a promising strategy to enhance the clinical efficacy of AZA in AML patients. This combination treatment is expected to exert cell-autonomous effects on AML cells by inducing their differentiation and apoptosis and cell-extrinsic effects by triggering an anti-leukemic immune response.

References

1. Saultz JN, Garzon R. Acute Myeloid Leukemia: A Concise Review. J Clin Med. 2016;5(3):33.
2. Ahmadmehrabi K, Haque AR, Aleem A, Griffiths EA, Roloff GW. Targeted Therapies for the Evolving Molecular Landscape of Acute Myeloid Leukemia. Cancers (Basel). 2021;13(18):4646.
3. Ciotti G, Marconi G, Martinelli G. Hypomethylating Agent-Based Combination Therapies to Treat Post-Hematopoietic Stem Cell Transplant Relapse of Acute Myeloid Leukemia. Front Oncol. 2022;11:810387.
4. Liu JCY, Kühbacher U, Larsen NB, et al. Mechanism and function of DNA replication-independent DNA-protein crosslink repair via the SUMO-RNF4 pathway. EMBO J. 2021;40(18):e107413.
5. Lund K, Cole JJ, VanderKraats ND, et al. DNMT inhibitors reverse a specific signature of aberrant promoter DNA methylation and associated gene silencing in AML. Genome Biol. 2014;15(8):406.
6. Dombret H, Seymour JF, Butrym A, et al. International phase 3 study of azacitidine vs conventional care regimens in older patients with newly diagnosed AML with >30% blasts. Blood. 2015;126(3):291-299.
7. DiNardo CD, Pratz K, Pullarkat V, et al. Venetoclax combined with decitabine or azacitidine in treatment-naive, elderly patients with acute myeloid leukemia. Blood. 2019;133(1):7-17.
8. DiNardo CD, Jonas BA, Pullarkat V, et al. Azacitidine and Venetoclax in Previously Untreated Acute Myeloid Leukemia. N Engl J Med. 2020;383(7):617-629.
9. Garciaz S, Saillard C, Hicheri Y, Hospital M-A, Vey N. Venetoclax in Acute Myeloid Leukemia: Molecular Basis, Evidences for Preclinical and Clinical Efficacy and Strategies to Target Resistance. Cancers. 2021;13(22):5608.
10. Ong F, Kim K, Konopleva MY. Venetoclax resistance: mechanistic insights and future strategies. Cancer Drug Resist. 2022;5(2):380-400.
11. Vertegaal ACO. Signalling mechanisms and cellular functions of SUMO. Nat Rev Mol Cell Biol. 2022;23(11):715-731.
12. Hendriks IA, Lyon D, Young C, Jensen LJ, Vertegaal ACO, Nielsen ML. Site-specific mapping of the human SUMO proteome reveals co-modification with phosphorylation. Nat Struct Mol Biol. 2017;24(3):325-336.
13. Hendriks IA, Lyon D, Su D, et al. Site-specific characterization of endogenous SUMOylation across species and organs. Nat Commun. 2018;9(1):2456.
14. Pichler A, Fatouros C, Lee H, Eisenhardt N. SUMO conjugation - a mechanistic view. Biomol Concepts. 2017;8(1):13-36.
15. Boulanger M, Chakraborty M, Tempé D, Piechaczyk M, Bossis G. SUMO and Transcriptional Regulation: The Lessons of Large-Scale Proteomic, Modifomic and Genomic Studies. Molecules. 2021;26(4):828.
16. Rosonina E. A conserved role for transcription factor sumoylation in binding-site selection. Curr Genet. 2019;65(6):1307-1312.
17. Bossis G, Sarry J-E, Kifagi C, et al. The ROS/SUMO Axis Contributes to the Response of Acute Myeloid Leukemia Cells to Chemotherapeutic Drugs. Cell Rep. 2014;7(6):1815-1823.
18. Baik H, Boulanger M, Hosseini M, et al. Targeting the SUMO Pathway Primes All-trans Retinoic Acid–Induced Differentiation of Nonpromyelocytic Acute Myeloid Leukemias. Cancer Res. 2018;78(10):2601-2613.
19. Langston SP, Grossman S, England D, et al. Discovery of TAK-981, a First-in-Class

Inhibitor of SUMO-Activating Enzyme for the Treatment of Cancer. J Med Chem. 2021;64(5):2501-2520.
20. Lightcap ES, Yu P, Grossman S, et al. A small-molecule SUMOylation inhibitor activates antitumor immune responses and potentiates immune therapies in preclinical models. Sci Transl Med. 2021;13(611):eaba7791.
21. Kumar S, Schoonderwoerd MJA, Kroonen JS, et al. Targeting pancreatic cancer by TAK-981: a SUMOylation inhibitor that activates the immune system and blocks cancer cell cycle progression in a preclinical model. Gut. 2022;71(11):2266-2283.
22. Demel UM, Böger M, Yousefian S, et al. Activated SUMOylation restricts MHC class I antigen presentation to confer immune evasion in cancer. J Clin Invest. 2022;132(9):e152383.
23. Nakamura A, Grossman S, Song K, et al. SUMOylation inhibitor subasumstat potentiates rituximab activity by IFN1-dependent macrophage and NK cell stimulation. Blood. 2022;139(18):2770-2781.
24. Demel UM, Wirth M, Yousefian S, et al. Small molecule SUMO inhibition for biomarker-informed B-cell lymphoma therapy. Haematologica. 2023;108(2):555-567.
25. Du L, Liu W, Pichiorri F, Rosen ST. SUMOylation inhibition enhances multiple myeloma sensitivity to lenalidomide. Cancer Gene Ther. 2022;30(4):567-574.
26. Du L, Liu W, Aldana-Masangkay G, et al. SUMOylation inhibition enhances dexamethasone sensitivity in multiple myeloma. J Exp Clin Cancer Res. 2022;41(1):1-16.
27. Kim HS, Kim B-R, Dao TTP, et al. TAK-981, a SUMOylation inhibitor, suppresses AML growth immune-independently. Blood Adv. 2023;7(13):3155-3168.
28. Paolillo R, Boulanger M, Gâtel P, et al. The NADPH oxidase NOX2 is a marker of adverse prognosis involved in chemoresistance of acute myeloid leukemias. Haematologica. 2022;107(11):2562-2575.
29. Gâtel P, Brockly F, Reynes C, et al. Ubiquitin and SUMO conjugation as biomarkers of acute myeloid leukemias response to chemotherapies. Life Sci Alliance. 2020;3(6):e201900577.
30. Recasens-Zorzo C, Gâtel P, Brockly F, Bossis G. A Microbead-Based Flow Cytometry Assay to Assess the Activity of Ubiquitin and Ubiquitin-Like Conjugating Enzymes. Methods Mol Biol. 2023;2602:65-79.
31. Gartel AL, Ye X, Goufman E, et al. Myc represses the p21(WAF1/CIP1) promoter and interacts with Sp1/Sp3. Proc Natl Acad Sci U S A. 2001;98(8):4510-4515.
32. Stubbins RJ, Karsan A. Differentiation therapy for myeloid malignancies: beyond cytotoxicity. Blood Cancer J. 2021;11(12):1-9.
33. Rahmani S, Yazdanpanah N, Rezaei N. Natural killer cells and acute myeloid leukemia: promises and challenges. Cancer Immunol Immunother. 2022;71(12):2849-2867.
34. Allende-Vega N, Marco Brualla J, Falvo P, et al. Metformin sensitizes leukemic cells to cytotoxic lymphocytes by increasing expression of intercellular adhesion molecule-1 (ICAM-1). Sci Rep. 2022;12(1):1341.
35. Carlsten M, Järås M. Natural Killer Cells in Myeloid Malignancies: Immune Surveillance, NK Cell Dysfunction, and Pharmacological Opportunities to Bolster the Endogenous NK Cells. Front Immunol. 2019;10:2357.
36. Seeler J-S, Dejean A. SUMO and the robustness of cancer. Nat Rev Cancer. 2017;17(3):184-197.
37. Boulanger M, Paolillo R, Piechaczyk M, Bossis G. The SUMO Pathway in Hematomalignancies and Their Response to Therapies. Int J Mol Sci. 2019;20(16):3895.
38. Zhou P, Chen X, Li M, et al. 2-D08 as a SUMOylation inhibitor induced ROS accumulation mediates apoptosis of acute myeloid leukemia cells possibly through the deSUMOylation of NOX2. Biochem Biophys Res Commun. 2019;513(4):1063-1069.

39. Benoit YD, Mitchell RR, Wang W, et al. Targeting SUMOylation dependency in human cancer stem cells through a unique SAE2 motif revealed by chemical genomics. Cell Chem Biol. 2021;28(10):1394-1406.
40. Ishii H, Yano S. New Therapeutic Strategies for Adult Acute Myeloid Leukemia. Cancers (Basel). 2022;14(11):2806.
41. Pei S, Pollyea DA, Gustafson A, et al. Monocytic Subclones Confer Resistance to Venetoclax-Based Therapy in Patients with Acute Myeloid Leukemia. Cancer Discov. 2020;10(4):536-551.
42. Ryu H-Y, Hochstrasser M. Histone sumoylation and chromatin dynamics. Nucleic Acids Res. 2021;49(11):6043-6052.
43. Seifert A, Schofield P, Barton GJ, Hay RT. Proteotoxic stress reprograms the chromatin landscape of SUMO modification. Sci Signal. 2015;8(384):rs7.
44. González-Prieto R, Eifler-Olivi K, Claessens LA, et al. Global non-covalent SUMO interaction networks reveal SUMO-dependent stabilization of the non-homologous end joining complex. Cell Rep. 2021;34(4):108691.
45. Lascorz J, Codina-Fabra J, Reverter D, Torres-Rosell J. SUMO-SIM interactions: From structure to biological functions. Semin Cell Dev Biol. 2022;132:193-202.
46. Ouyang J, Shi Y, Valin A, Xuan Y, Gill G. Direct binding of CoREST1 to SUMO-2/3 contributes to gene-specific repression by the LSD1/CoREST1/HDAC complex. Mol Cell. 2009;34(2):145-154.
47. Hua G, Ganti KP, Chambon P. Glucocorticoid-induced tethered transrepression requires SUMOylation of GR and formation of a SUMO-SMRT/NCoR1-HDAC3 repressing complex. Proc Natl Acad Sci U S A. 2016;113(5):E635-E643.
48. Pascual G, Fong AL, Ogawa S, et al. A SUMOylation-dependent pathway mediates transrepression of inflammatory response genes by PPAR-γ. Nature. 2005;437(7059):759-763.
49. Ivanov AV, Peng H, Yurchenko V, et al. PHD Domain-Mediated E3 Ligase Activity Directs Intramolecular Sumoylation of an Adjacent Bromodomain Required for Gene Silencing. Mol Cell. 2007;28(5):823-837.
50. Boulanger M, Aqrouq M, Tempé D, et al. DeSUMOylation of chromatin-bound proteins limits the rapid transcriptional reprogramming induced by daunorubicin in acute myeloid leukemias. Nucleic Acids Res. 2023 Jul 18. [Epub ahead of print]
51. Borgermann N, Ackermann L, Schwertman P, et al. SUMOylation promotes protective responses to DNA-protein crosslinks. EMBO J. 2019;38(8):e101496.
52. Kroonen JS, de Graaf IJ, Kumar S, et al. Inhibition of SUMOylation enhances DNA hypomethylating drug efficacy to reduce outgrowth of hematopoietic malignancies. Leukemia. 2023;37(4):864-876.
53. Hollenbach PW, Nguyen AN, Brady H, et al. A Comparison of Azacitidine and Decitabine Activities in Acute Myeloid Leukemia Cell Lines. PLoS One. 2010;5(2):e9001.
54. Yilmaz M, Kantarjian H, Ravandi F. Acute promyelocytic leukemia current treatment algorithms. Blood Cancer J. 2021;11(6):1-9.
55. Madan V, Koeffler HP. Differentiation therapy of myeloid leukemia: four decades of development. Haematologica. 2021;106(1):26-38.
56. Roulois D, Loo Yau H, Singhania R, et al. DNA-Demethylating Agents Target Colorectal Cancer Cells by Inducing Viral Mimicry by Endogenous Transcripts. Cell. 2015;162(5):961-973.
57. Chiappinelli KB, Strissel PL, Desrichard A, et al. Inhibiting DNA Methylation Causes an Interferon Response in Cancer via dsRNA Including Endogenous Retroviruses. Cell. 2015;162(5):974-986.
58. Aricò E, Castiello L, Capone I, Gabriele L, Belardelli F. Type I Interferons and

Cancer: An Evolving Story Demanding Novel Clinical Applications. Cancers (Basel). 2019;11(12):1943.

Figure legend

Figure 1: TAK981 synergizes with AZA to induce AML cell death *in vitro*

A) HL-60 cells were treated with increasing doses of TAK-981 for 24 hours and immunoblotted for SUMO-1, SUMO-2/3 and GAPDH. SUMO conjugates appear as smears **B)** TAK-981 IC_{50} (half-maximal inhibitory concentration) were determined using HL-60, U937 and THP-1 cells treated with varying drug concentrations. Cell viability was determined using MTS assays after 24 hours of treatment. Concentration-response curves were generated by comparing the viability of TAK-981 treated cells with mock-treated controls. Data are shown as mean +/- SEM of replicate samples (n = 5). Absolute IC_{50} are indicated on the figure. **C)** BMMC (n = 2) and PBMC (n = 3) collected from healthy donors were treated with varying TAK-981 concentrations for 24 hours. Cell viability was determined by flow cytometry after 24 hours of treatment. Concentration-response curves were generated by comparing the viability of TAK-981 treated cells with mock-treated controls. Data are shown as mean +/- SEM of replicate samples. **D)** HL-60 cells were treated for 24 hours with TAK-981 and either DNR, ARA-C or AZA and viability was assessed by MTS assay (median of 3 independent experiments for each drug). Left panels: heat maps showing the synergy ZIP-score between the two drugs, and the "most synergistic areas" (black squares) estimated using the SynergyFinder software v2.0. Right panel: Mean of synergy ZIP-scores in most synergistic areas for HL-60 cells. Data are shown as mean +/- SD of replicate samples (n = 3 for each drug). Dotted line at 10% represents the threshold for significant synergy. **E)** HL-60, U937 and THP-1 cells were treated with TAK-981 and AZA every day for 3 consecutive days. Viability was analyzed at day 4 and compared to that in mock-treated conditions (median of 3 independent experiments for each cell line). Left panels: heat maps for the corresponding

synergy ZIP-score between the TAK-981 and AZA, and the "most synergistic areas" (black squares) estimated using the SynergyFinder software v2.0. Right panel: Mean of synergy ZIP-scores in most synergistic areas for the 3 cell lines. Data are shown as mean +/- SD of replicate samples (n = 3 for each cell line). Dotted line at 10% represents the threshold for significant synergy. **F,G)** Patient (n = 17) (F) or healthy donor (n = 6) (G) bone marrow mononuclear cells were treated for 3 consecutive days (Day 1, 2, 3) with TAK-981 (10 nM) and/or AZA (100 nM) and kept in culture. After 8 days, cells were collected and the number of CD45+ cells was analyzed by flow cytometry in each condition and compared to the mock-treated condition. For each group, plain lines represent the median value, and dotted lines are the quartiles. Groups were compared using RM one-way ANOVA test.

Figure 2: TAK-981 and AZA combination has a higher anti-leukemic activity than monotherapies *in vivo*

A,B) NSG mice were injected with THP-1 cells and treated with TAK-981 (15 mg/kg, IV), AZA (2 mg/kg, IP) or the combination according to the schedule presented in Supplementary Figure 2B (n=5/group). **A)**. Quantification, as relative luminescence units, of tumor burden evolution monitored by luminescence intensity in mice injected with bioluminescent THP-1 cells. **B)** Overall survival after treatment start of mice injected with bioluminescent THP-1 cells was estimated in each group and compared using Kaplan-Meier method and log-rank test. **C,D)** NSG mice were injected with THP-1 cells and treated with TAK-981 (15 mg/kg, IV) and AZA (2 mg/kg, IP) or VEN (50 mg/kg, OG) according to the schedule presented in Supplementary Figure 2D (n=7/group). **C)** Quantification (as relative luminescence units) of tumor burden evolution monitored by luminescence intensity in mice injected with bioluminescent THP-1 cells. **D)** Overall survival after treatment start of mice injected with

bioluminescent THP-1 cells was estimated in each group of treatment and compared using Kaplan-Meier method and log-rank test. **E,F)** NSG mice were injected with primary cells from 2 different AML patients. After engraftment, mice were treated with AZA and/or TAK-981 and euthanized at day 9. The total number of human CD45+ cells (hCD45) was estimated by flow cytometry in bone marrow (PDX#1, n=7) and spleen (PDX#1, n=6; PDX#2, n=4 to 6), and compared to the mean number of cells collected in the mock-treated group of mice. For each group, plain lines represent the median value, and dotted lines are the quartiles. Groups were compared using Ordinary one-way ANOVA test.

Figure 3: TAK-981 enhances AZA-induced transcriptional reprogramming in U937 AML cell line

A, B, C) Volcano plots showing differentially expressed genes (DEG) in U937 cell line treated each day for 3 days with AZA (10 nM; A), TAK-981 (10 nM; B) or the combination TAK-981+AZA (10 nM each; C), analyzed at day 4 by RNA-Seq and compared to mock-treated cells (n=3). Red dotted lines indicate the two-fold change cut-off (abs(log_2FC)= 1) and a p-value of 0.05 (log_{10} = 1.3). The total numbers of up- and down-DEGs are indicated. Orange and violet dots indicate genes whose expression is respectively up- or down-regulated more than 2-fold by AZA-alone treatment. **D)** Scatter plot displaying the DESeq2 fold change of DEGs in TAK-981+AZA treated U937 cells as a function of their fold change in AZA-treated cells. The red line represents the linear regression of the fold changes for the comparison of AZA+TAK-981 vs. AZA replicates. As a control, the grey line represents the linear regression from the comparison of AZA vs. AZA replicates. P-value was calculated using student t-test between the two linear regressions. E) GSEA were performed using Hallmark datasets on the RNA-Seq data obtained from U937 cells. All pathways significantly enriched in the AZA + TAK-981

compared to mock-treated cells are shown (abs(NES)>1, p<0.05 and FDR<0.05). NES and FDR are also indicated for the AZA and TAK-981 vs mock-treated cells.

Figure 4: TAK-981+ AZA induces apoptosis and cell cycle defects in AML cells

A) U937 or THP1 cells were treated every day for 3 consecutive days with TAK-981, AZA or VEN at the indicated doses and stained on day 4 with Annexin-V/7AAD to quantify apoptotic and dead cells (n=3, mean +/- SD, conditions were compared to mock-treated condition using ordinary one-way Anova). **B)** Cells treated as in A were stained with propidium iodide to analyze cell cycle distribution (n=3, mean +/- SD).

Figure 5: TAK-981+ AZA induces differentiation of AML cells

A) GSEA enrichment plot for the gene signature "GOBP Myeloid Cell Differentiation" in TAK-981+AZA-treated U937 cells compared to mock- (upper panel) or AZA- (lower panel) treated cells. **B)** mRNA expression of *CD14* was analyzed by qRT-PCR in U937 cells treated for 72 hours with 10 nM AZA, 10 nM TAK-981 or the drug combination. Results were normalized to *GAPDH* mRNA levels and expressed as ratio to mock-treated cells (n=3, mean +/- SD, conditions were compared using RM one-way ANOVA test). **C)** NSG mice were injected with U937 cells (n=4 or 5/group) and, after engraftment, treated according to treatment schedule presented in Figure 2A. Bone marrow were collected at day 9 after treatment start and the level of CD14 was assessed by flow cytometry at cell surface of hCD45+ cells. Data were normalized to the mean of CD14 expression (MFI) in mock-treated group of mice. For each group, plain lines represent the median value and dotted lines are the quartiles. Groups were compared using Ordinary one-way ANOVA test. **D)** Expression of CD14 was measured by flow cytometry on THP-1 treated with 10 nM AZA, 10 nM TAK-981 or the drug

combination for 72 hours. MFI were normalized to that of mock-treated cells (n=6, mean +/- SD, RM one-way ANOVA test). **E, F)** NSG mice were injected with primary patient cells (PDX#1), and treated according to treatment schedule presented in Figure 2A. Peripheral blood samples (n=3 to 6/group) were collected at day 30 after treatment start (E) or, in an independent experiment, spleens (n=6 or 7/group) were collected at day 9 after treatment start (F). The level of CD14 and CD15 protein expression at cell surface of hCD45+ cells was evaluated by flow cytometry. Data were normalized on the mean of CD14 and CD15 expression (MFI) in cells from the mock-treated group. For each group, plain lines represent the median values, and dotted lines are the quartiles. Groups were compared using Kruskall-Wallis test, due to lack of normality of data.

Figure 6: TAK-981 and AZA combination activates IFN-I secretion by AML cells

A) GSEA enrichment plot for genes involved in IFN-α response in TAK-981+AZA treated U937 cells compared to mock- (upper panel) and AZA- (lower panel) treated cells. **B)** Heatmap representing the RNAseq results for the expression of IRFs in U937 cells. **C, D)** mRNA expression of *IRF7* (C) and *IRF9* (D) was analyzed by qRT-PCR in THP-1 cells treated for 72 hours with 10 nM TAK-981 and the indicated concentrations of AZA. Results were normalized to *GAPDH* mRNA levels and expressed as ratio to mock-treated cells (n=3 to 5, mean +/- SD, all conditions were compared using RM one-way ANOVA test, only those with significant p-values are shown). **E)** THP-1 cells were treated for 3 consecutive days with TAK-981 (10 nM) and/or AZA (10nM or 100 nM). After 8 days, cells were collected and the production of intracellular IFN-α was analyzed by flow cytometry. Background was subtracted and data normalized to the mock-treated condition (n=3, mean +/- SD, all conditions were compared using RM one-way ANOVA test, only those with significant p-

values are shown). **F)** NSG mice were injected with primary patient cells (PDX#1) and treated according to treatment schedule presented in Figure 2A. Spleens (n=6/group) were collected at day 9 after treatment start and the level of intra-cellular IFN-α in hCD45+ cells was assessed by flow cytometry. Data were normalized to the mean of IFN-α expression (MFI) in mock-treated group of mice. For each group, plain lines represent the median value and dotted lines are the quartiles. Groups were compared using Ordinary one-way ANOVA test.

Figure 7: TAK-981 treatment of AML cells leads to NK cells activation and increased NK cytotoxicity

A) GSEA enrichment plot for genes involved in NK-mediated cytotoxicity in TAK-981+AZA treated U937 cells compared to mock- (upper panel) or AZA- (lower panel) treated cells. **B, C)** Expression of ICAM-1 (B) and MICA/B (C) was measured by flow cytometry on THP-1 treated with 10 nM TAK-981 and AZA at the indicated concentrations for 72 hours. Background was subtracted and results were normalized to mock-treated condition (n=10 for ICAM-1, n=5 for MICA/B, mean +/- SD, RM one-way ANOVA test). **D, E)** NSG mice (n=7/group) were injected with primary patient cells (PDX #1), and treated according to treatment schedule presented in Figure 2A. Bone marrows were collected at day 9 after treatment start and ICAM-1 and MICA/B expression on the membrane of human CD45+ cells was assessed by flow cytometry. Data were normalized to the mean MFI of mock-treated mice group. Plain lines represent the median values, and dotted lines are the quartiles. Groups were compared using Kruskall-Wallis test. **F)** THP-1 cells were treated each day for 3 consecutive days with 10nM AZA, 10nM TAK-981 or the drug combination, and cocultured at day 8 with healthy donor PBMC at a 1:10 AML:PBMC ratio. After 24 hours of coculture, expression of activation marker CD69 was assessed by flow cytometry on NK cells (CD3-

/CD56+ cells). Data were normalized to the MFI of CD69 expression on NK cells co-cultured with untreated THP-1, (mean +/- SD, n = 6, RM one-way ANOVA test). **G, H)** Real-time immune cell killing assay. To evaluate NK cell cytotoxicity against AML cells treated with TAK-981 -/+ AZA, coculture experiments were performed during 15 hours using an Incucyte device between, on one hand, THP-1-LucZsGreen cells previously treated for 72 hours with 10 nM AZA, 10 nM TAK-981 or the drug combination, and on the other hand, NK cells, purified from healthy donor PBMC. Cells were used at a 1:1 AML:NK ratio. **G)** Relative green fluorescence intensities for THP-1-LucZsGreen cells mock-treated without (grey curve) or with NK cells (light blue curve) and treated with TAK-981+AZA without (red curve) or with NK cells (dark blue curve) (n = 5). Cytotoxicity of NK cells was calculated by comparing grey- (mock-treated THP-1 -/+ NK cells) and red areas (AZA+TAK-981 treated THP-1 -/+ NK cells). **H)** NK cells cytotoxicity was determined by calculating areas between the curves for each treatment condition (10 nM AZA, 10 nM TAK-981 or the drug combination) with or without NK. Data were normalized to mock-treated THP-1 cells (n=5, mean +/- SD, RM one-way ANOVA test).

Figure 8: Model for the anti-leukemic activity of TAK-981+AZA in AML. Combined inhibition of SUMOylation with TAK-981 and DNA methylation with AZA induces a transcriptional reprogramming in AML cells. This includes the activation of genes involved in the induction of apoptosis and differentiation and a repression of genes linked to cell cycle progression. In addition, TAK-981+AZA induces IFN-I secretion as well as the expression of Natural Killer ligands at the surface of AML cells. This activates NK and increase their cytotoxicity towards AML cells.

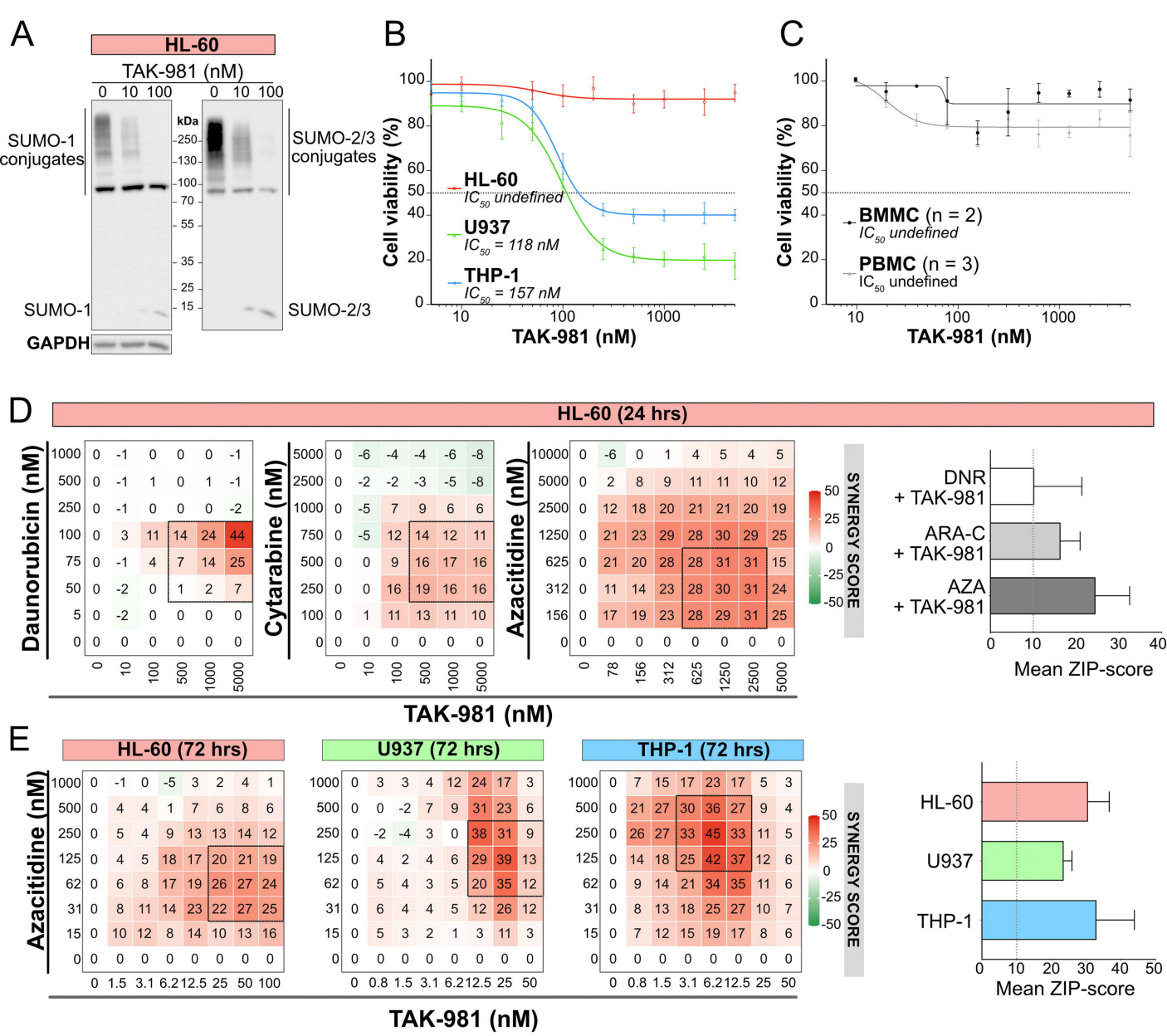
A
HL-60
TAK-981 (nM)
0 10 100 0 10 100
kDa
250
130
100
70
55
35
25
15
SUMO-1 conjugates
SUMO-2/3 conjugates
SUMO-1
SUMO-2/3
GAPDH
B
Cell viability (%)
HL-60
IC50 undefined
U937
IC50 = 118 nM
THP-1
IC50 = 157 nM
TAK-981 (nM)
C
Cell viability (%)
BMMC (n = 2)
IC50 undefined
PBMC (n = 3)
IC50 undefined
TAK-981 (nM)
D
HL-60 (24 hrs)
Daunorubicin (nM)
Cytarabine (nM)
Azacitidine (nM)
SYNERGY SCORE
DNR + TAK-981
ARA-C + TAK-981
AZA + TAK-981
Mean ZIP-score
TAK-981 (nM)
E
HL-60 (72 hrs)
U937 (72 hrs)
THP-1 (72 hrs)
Azacitidine (nM)
SYNERGY SCORE
HL-60
U937
THP-1
Mean ZIP-score
TAK-981 (nM)
F
AML patient cells
CD45+ blast cells (% of mock condition)
Mock
AZA
TAK-981
TAK-981 +AZA
G
Healthy donors BMMC
CD45+ cells (% of mock condition)
Mock
AZA
TAK-981
TAK-981 +AZA

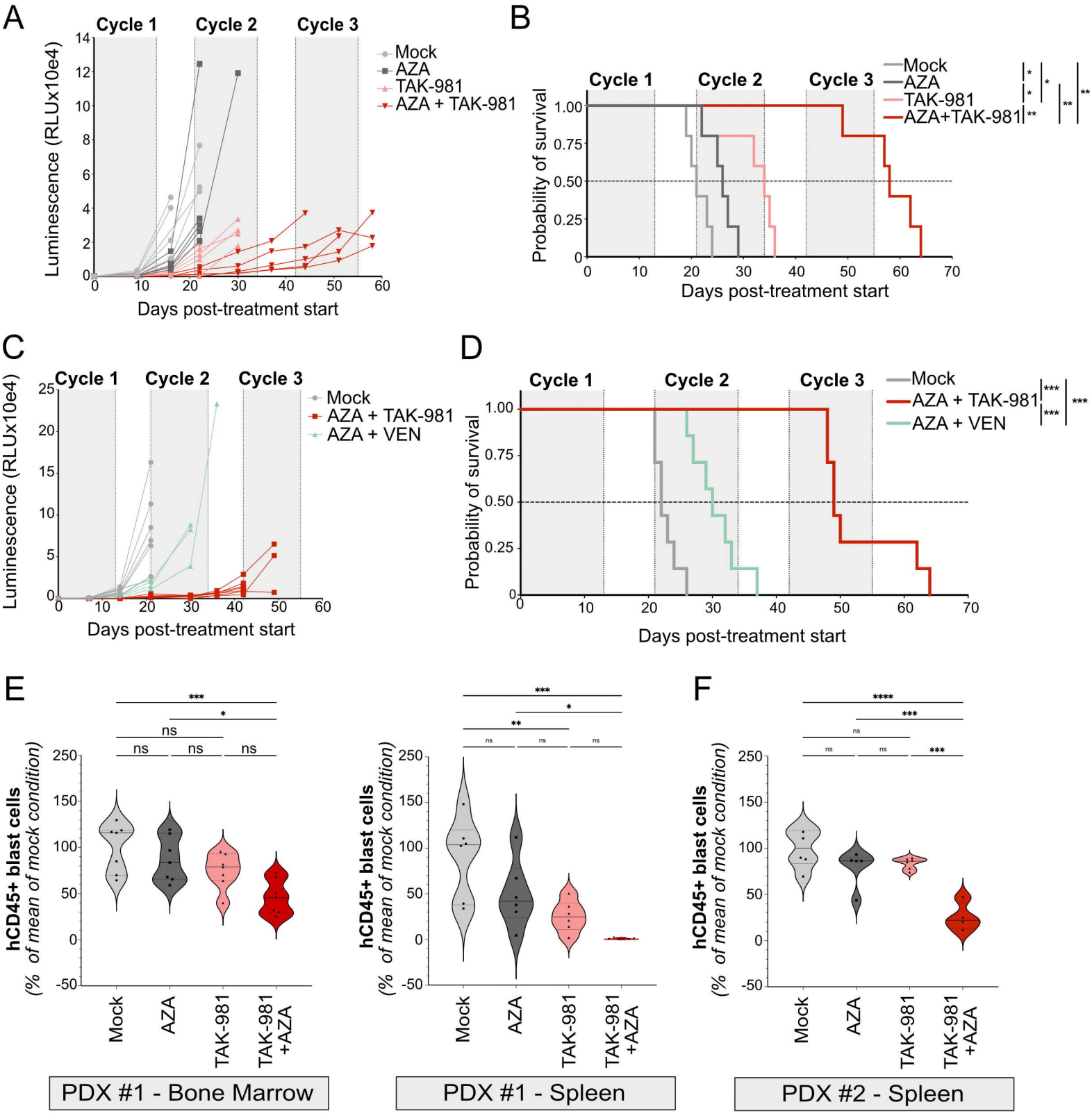
A
Cycle 1
Cycle 2
Cycle 3
Luminescence (RLUx10e4)
Days post-treatment start
Mock
AZA
TAK-981
AZA + TAK-981
B
Probability of survival
Days post-treatment start
AZA+TAK-981
C
AZA + VEN
D
E
F
hCD45+ blast cells
(% of mean of mock condition)
ns
Mock
TAK-981
TAK-981 +AZA
PDX #1 - Bone Marrow
PDX #1 - Spleen
PDX #2 - Spleen

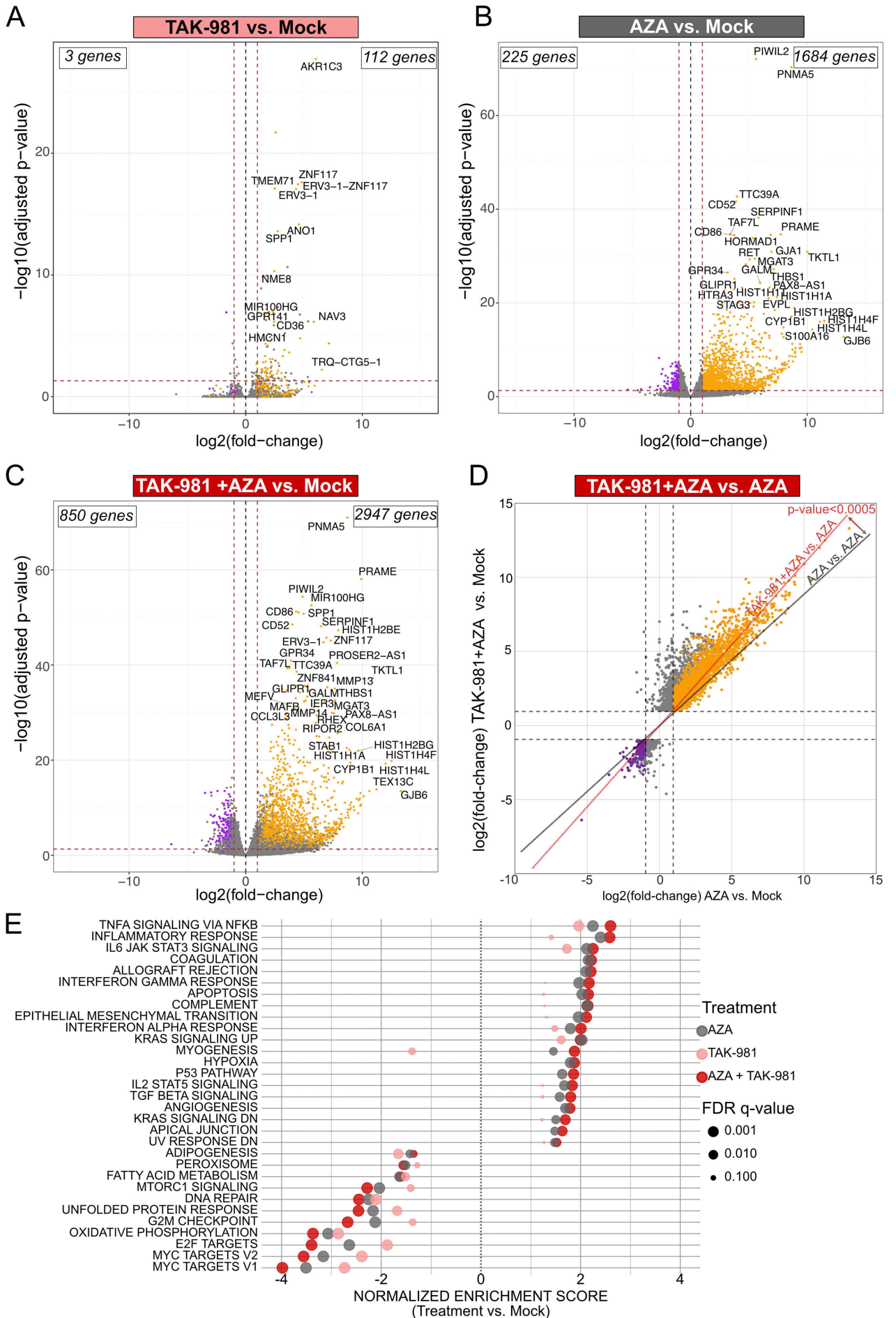
A
TAK-981 vs. Mock
3 genes
112 genes
AKR1C3
ZNF117
TMEM71
ERV3−1−ZNF117
ERV3−1
ANO1
SPP1
NME8
MIR100HG
GPR141
NAV3
CD36
HMCN1
TRQ−CTG5−1
−log10(adjusted p−value)
log2(fold−change)
B
AZA vs. Mock
225 genes
1684 genes
PIWIL2
PNMA5
TTC39A
CD52
SERPINF1
TAF7L
PRAME
CD86
HORMAD1
RET
GJA1
MGAT3
TKTL1
GPR34
GALM
THBS1
PAX8−AS1
GLIPR1
HTRA3
HIST1H1
HIST1H1A
STAG3
EVPL
HIST1H2BG
CYP1B1
HIST1H4F
HIST1H4L
S100A16
GJB6
C
TAK-981 +AZA vs. Mock
850 genes
2947 genes
PNMA5
PRAME
PIWIL2
MIR100HG
CD86
SPP1
SERPINF1
CD52
HIST1H2BE
ERV3−1
ZNF117
GPR34
PROSER2−AS1
TAF7L
TTC39A
TKTL1
ZNF841
MMP13
GLIPR1
GALM
THBS1
MEFV
MAFB
IER3
MGAT3
CCL3L3
MMP14
PAX8−AS1
RHEX
RIPOR2
COL6A1
STAB1
HIST1H2BG
HIST1H1A
HIST1H4F
CYP1B1
HIST1H4L
TEX13C
GJB6
D
TAK-981+AZA vs. AZA
p-value<0.0005
TAK-981+AZA vs. AZA
AZA vs. AZA
log2(fold-change) TAK-981+AZA vs. Mock
log2(fold-change) AZA vs. Mock
E
TNFA SIGNALING VIA NFKB
INFLAMMATORY RESPONSE
IL6 JAK STAT3 SIGNALING
COAGULATION
ALLOGRAFT REJECTION
INTERFERON GAMMA RESPONSE
APOPTOSIS
COMPLEMENT
EPITHELIAL MESENCHYMAL TRANSITION
INTERFERON ALPHA RESPONSE
KRAS SIGNALING UP
MYOGENESIS
HYPOXIA
P53 PATHWAY
IL2 STAT5 SIGNALING
TGF BETA SIGNALING
ANGIOGENESIS
KRAS SIGNALING DN
APICAL JUNCTION
UV RESPONSE DN
ADIPOGENESIS
PEROXISOME
FATTY ACID METABOLISM
MTORC1 SIGNALING
DNA REPAIR
UNFOLDED PROTEIN RESPONSE
G2M CHECKPOINT
OXIDATIVE PHOSPHORYLATION
E2F TARGETS
MYC TARGETS V2
MYC TARGETS V1
NORMALIZED ENRICHMENT SCORE
(Treatment vs. Mock)
Treatment
AZA
TAK-981
AZA + TAK-981
FDR q-value
0.001
0.010
0.100

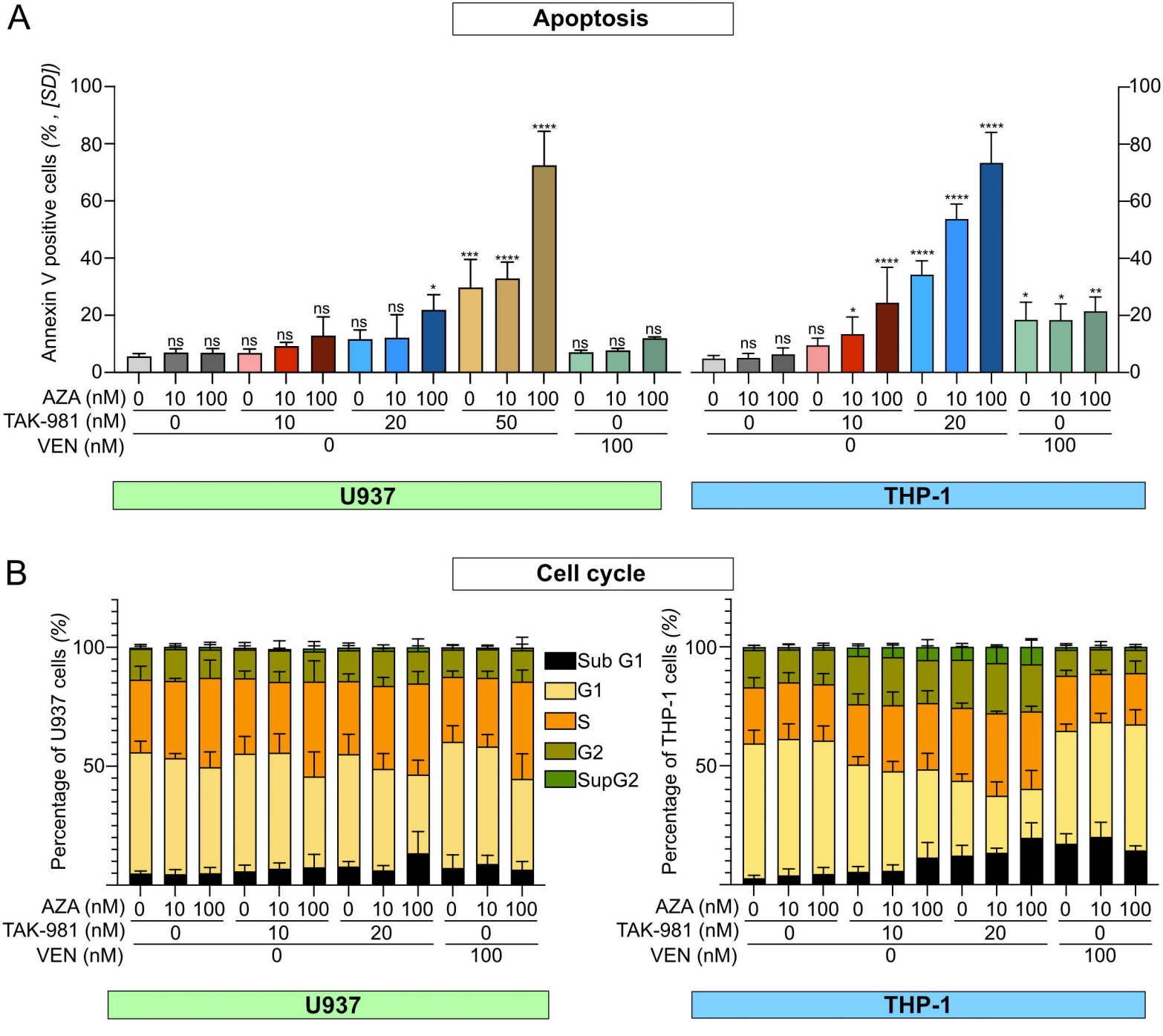
A
Apoptosis
Annexin V positive cells (% , [SD])
AZA (nM)
TAK-981 (nM)
VEN (nM)
U937
THP-1
B
Cell cycle
Percentage of U937 cells (%)
Percentage of THP-1 cells (%)
Sub G1
G1
S
G2
SupG2

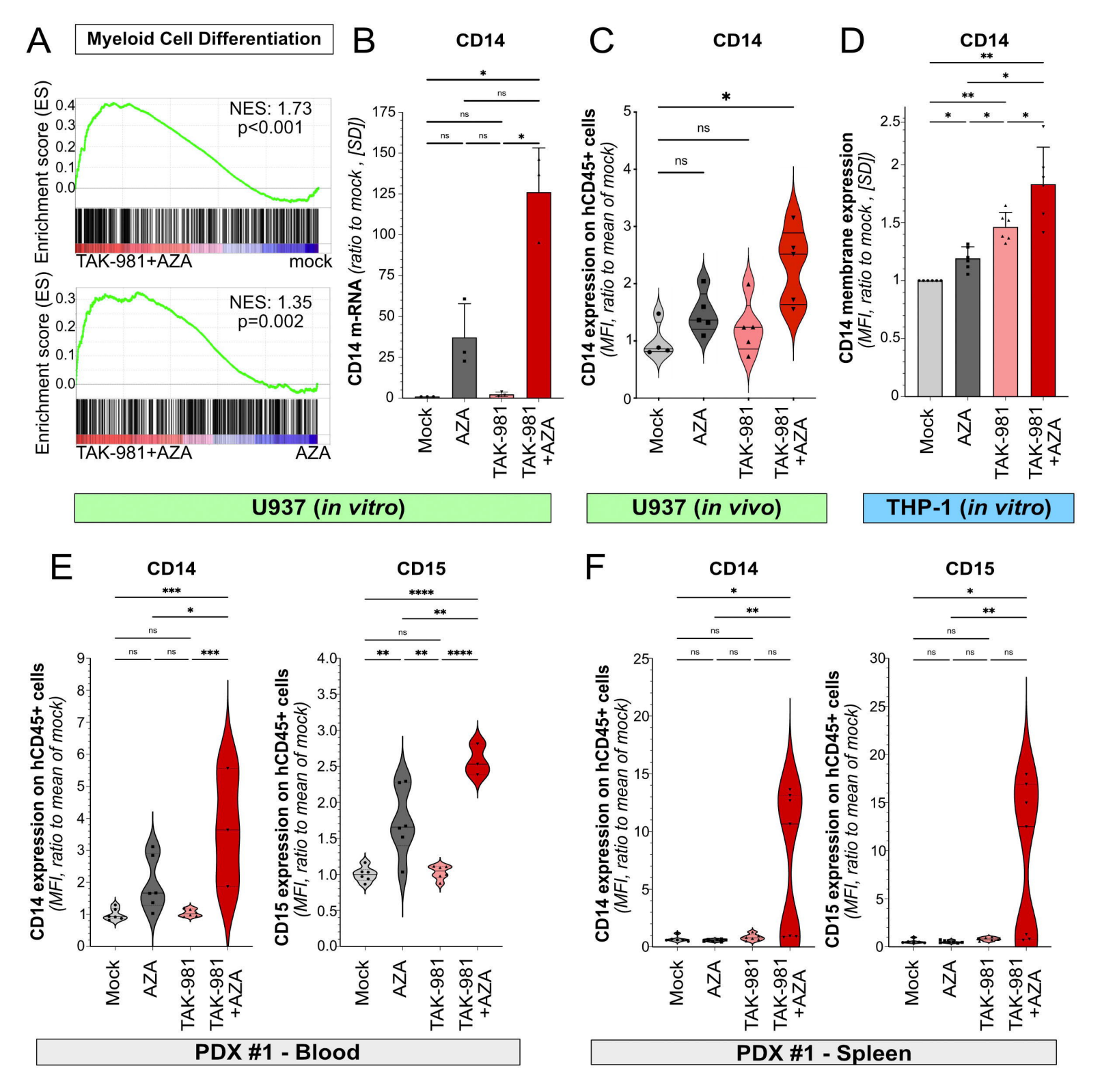
A
Myeloid Cell Differentiation
Enrichment score (ES)
NES: 1.73
p<0.001
TAK-981+AZA
mock
NES: 1.35
p=0.002
TAK-981+AZA
AZA
B
CD14
CD14 m-RNA (ratio to mock , [SD])
Mock
AZA
TAK-981
TAK-981 +AZA
C
CD14
CD14 expression on hCD45+ cells (MFI, ratio to mean of mock)
D
CD14
CD14 membrane expression (MFI, ratio to mock , [SD])
U937 (in vitro)
U937 (in vivo)
THP-1 (in vitro)
E
CD14
CD15
CD14 expression on hCD45+ cells (MFI, ratio to mean of mock)
CD15 expression on hCD45+ cells (MFI, ratio to mean of mock)
PDX #1 - Blood
F
CD14
CD15
PDX #1 - Spleen

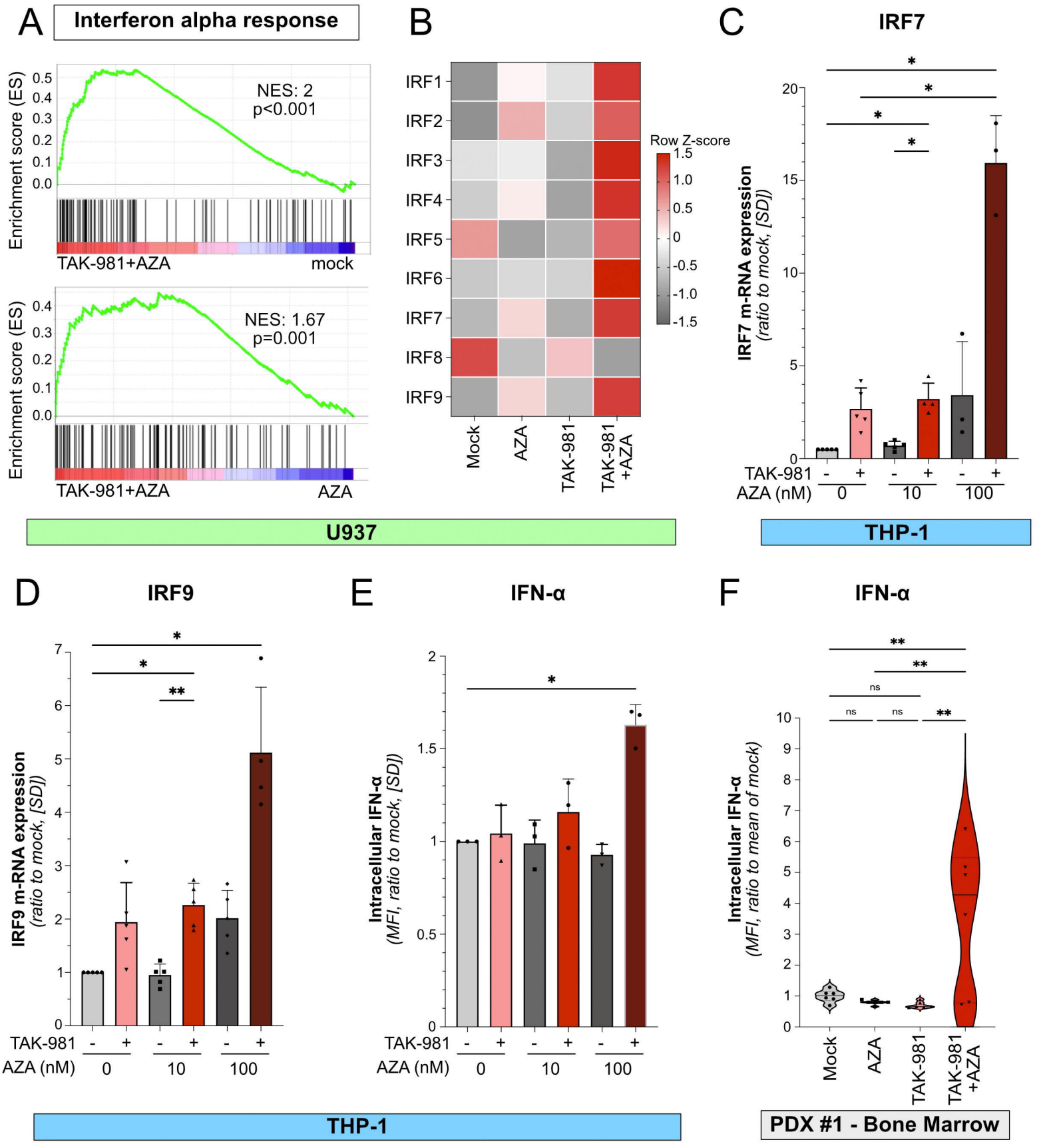
A
Interferon alpha response
Enrichment score (ES)
NES: 2
p<0.001
TAK-981+AZA
mock
NES: 1.67
p=0.001
AZA
B
IRF1
IRF2
IRF3
IRF4
IRF5
IRF6
IRF7
IRF8
IRF9
Row Z-score
Mock
AZA
TAK-981
TAK-981 +AZA
C
IRF7
IRF7 m-RNA expression
(ratio to mock, [SD])
TAK-981
AZA (nM)
U937
THP-1
D
IRF9
IRF9 m-RNA expression
(ratio to mock, [SD])
E
IFN-α
Intracellular IFN-α
(MFI, ratio to mock, [SD])
F
IFN-α
Intracellular IFN-α
(MFI, ratio to mean of mock)
ns
THP-1
PDX #1 - Bone Marrow

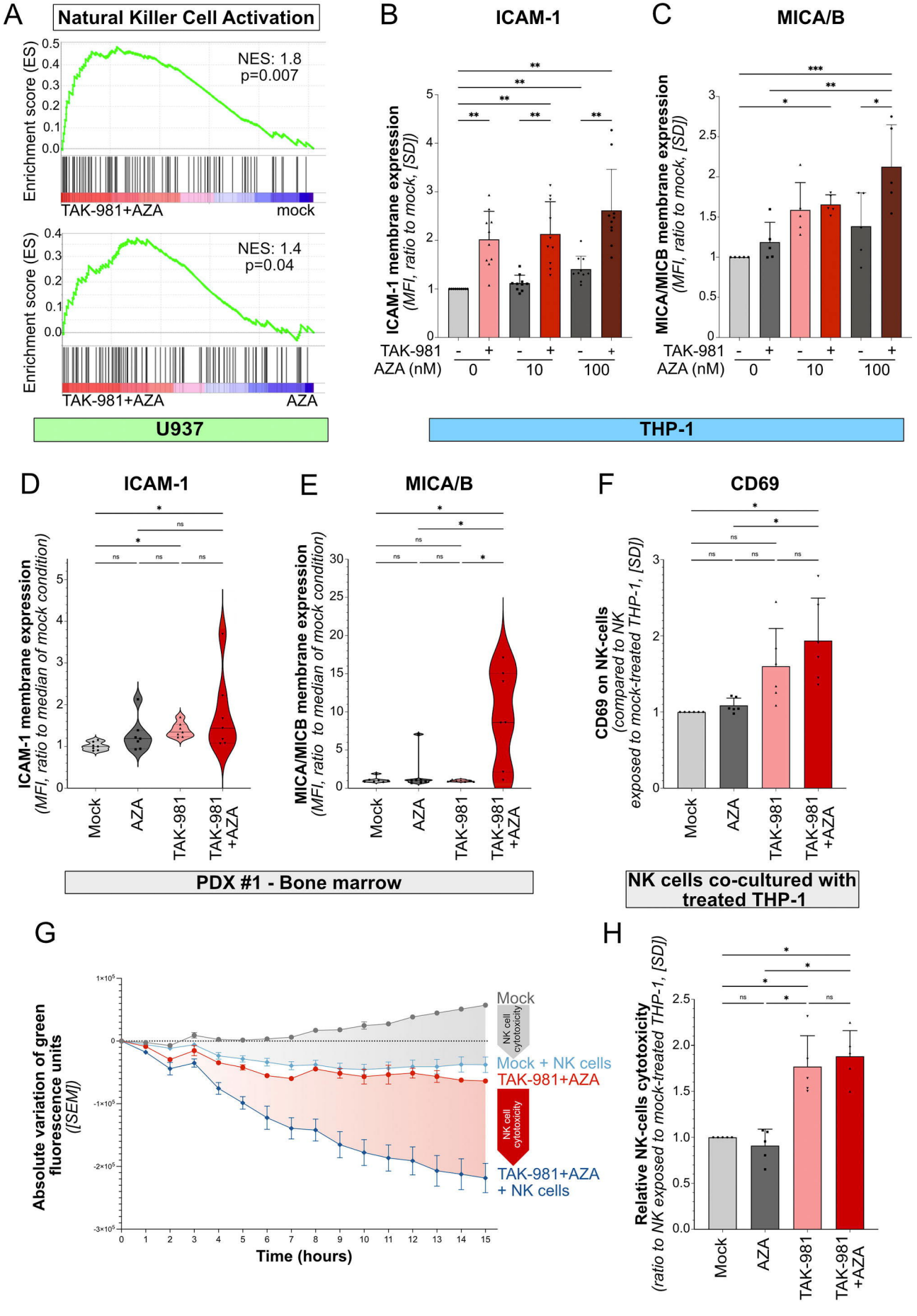
A
Natural Killer Cell Activation
Enrichment score (ES)
NES: 1.8
p=0.007
TAK-981+AZA
mock
NES: 1.4
p=0.04
AZA
U937
B
ICAM-1
ICAM-1 membrane expression
(MFI, ratio to mock, [SD])
TAK-981
AZA (nM)
0
10
100
C
MICA/B
MICA/MICB membrane expression
(MFI, ratio to mock, [SD])
THP-1
D
ICAM-1
ICAM-1 membrane expression
(MFI, ratio to median of mock condition)
Mock
AZA
TAK-981
TAK-981 +AZA
E
MICA/B
MICA/MICB membrane expression
(MFI, ratio to median of mock condition)
PDX #1 - Bone marrow
F
CD69
CD69 on NK-cells
(compared to NK exposed to mock-treated THP-1, [SD])
NK cells co-cultured with treated THP-1
G
Absolute variation of green fluorescence units
([SEM])
Time (hours)
Mock
NK cell cytotoxicity
Mock + NK cells
TAK-981+AZA
TAK-981+AZA + NK cells
H
Relative NK-cells cytotoxicity
(ratio to NK exposed to mock-treated THP-1, [SD])

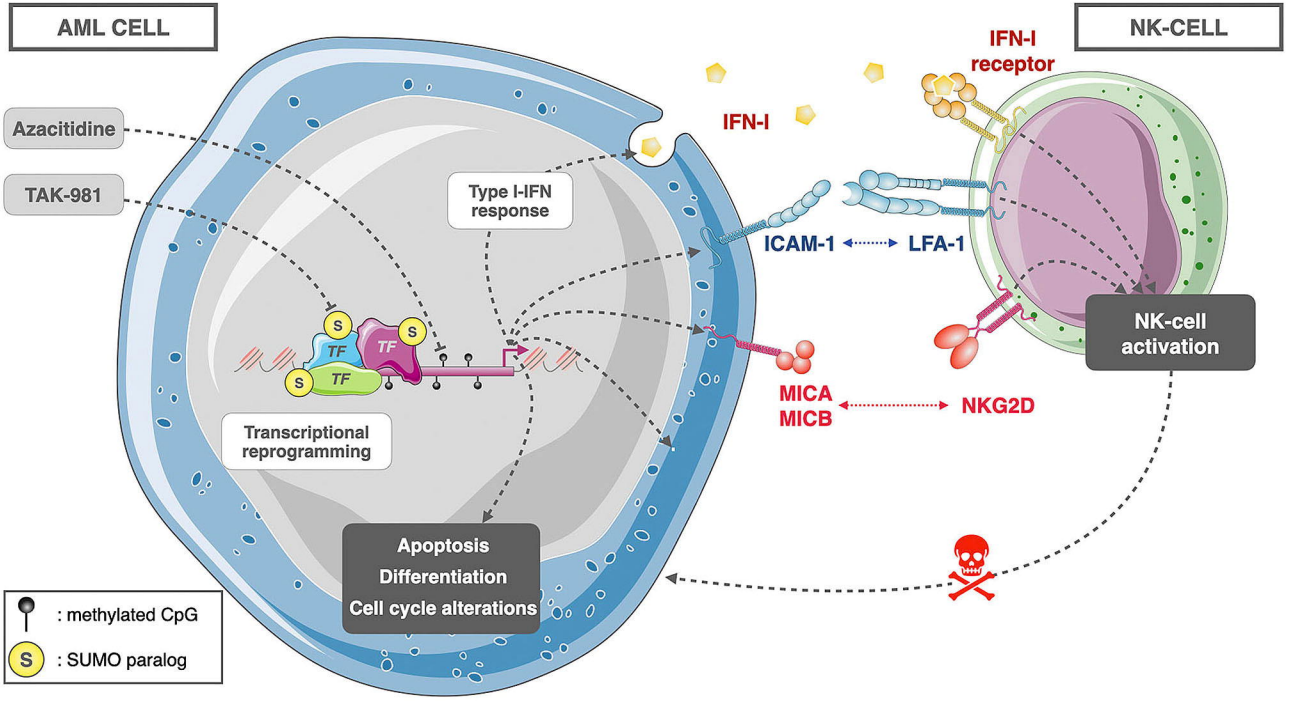
AML CELL
NK-CELL
Azacitidine
TAK-981
Type I-IFN response
IFN-I
IFN-I receptor
ICAM-1
LFA-1
NK-cell activation
MICA
MICB
NKG2D
S
TF
TF
S
S
TF
Transcriptional reprogramming
Apoptosis
Differentiation
Cell cycle alterations
: methylated CpG
S : SUMO paralog

Supplementary Methods

Generation of bioluminescent AML cell lines

THP-1-LucZsGreen and U937-LucZsGreen cell lines were obtained by retroviral gene transfer. Retroviruses were produced by cotransfection of HEK293T cells with the pHIV-Luc-ZsGreen (Addgene, Plasmid #39196), psPAX2 (Addgene, Plasmid #12260) and pCMV-VSV-G (Addgene, Plasmid #8454) vectors using Lipofectamine 2000 (Invitrogen). Viral supernatants were collected 48 hours after transfection, 0.45 µm-filtered, and used to infect AML cell lines. Two weeks after infection, ZsGreen-positive cells were cloned using a FACSAria cell sorter (Becton Dickinson).

Patient cells culture

Immediately after collection, fresh leukocytes were purified by density-based centrifugation using Histopaque 1077 (Sigma-Aldrich), frozen and stored in liquid nitrogen. After thawing, leukocytes were cultured in the StemSpan SFEM II culture medium (StemCell Technologies), supplemented with StemSpan CD34+ expansion supplement and UM729 according to supplier's recommendations. Cells were collected and analyzed after 8 days of culture.

IC_{50} measurement and synergy matrices

For 24 hours IC_{50} measurements, medium was complemented with drugs and analyzed 24 hours later. For 72 hours IC_{50} measurements, cells were treated on day 1 and 2. Cells were diluted twice on day 3 and treated with drugs and cell viability was analyzed 24 hours later. Cell viability was measured using the MTS viability assay (Promega) according to supplier's protocol. For PBMC, which metabolize MTS poorly, cell viability was measured by flow cytometry using FSC/SSC gating to select living cells. Absolute IC_{50} were calculated using the GraphPad PRISM software (version 9). Zero-interaction potency (ZIP) score gives a measure of drug interaction relationship by comparing the change in the potency of the dose-response curves between individual drugs and their combinations. ZIP score was calculated using online SynergyFinder software v2.0 (https://synergyfinder.fimm.fi)[1].

Immunoblots

Equal number of cells were collected and directly lysed in Laemmli electrophoresis sample buffer. Antibodies against SUMO-1 (21C7), and SUMO-2/3 (8A2) were obtained from the Developmental Studies Hybridoma Bank.

Flow cytometry

Cells were washed in PBS containing 5% FBS, incubated at 4°C for 30 minutes with conjugated antibodies (see Table 1), washed with PBS and analyzed by flow cytometry with a Novocyte flow cytometer (Agilent). Median fluorescence intensities (MFI) or the percentages of positive cells were calculated using the NovoExpress software (v.1.5.6). For the experiments with mice, bone marrows (from tibias and femurs) and spleens were dissociated and cells were rinsed in PBS. After red blood cells lysis using the ACK lysis buffer (A1049201, Gibco), mononuclear cells from bone marrow and spleen were labeled as described above. Anti-hCD45 antibodies were used to identify human blasts as CD45 is expressed on human leukocytes. For cell cycle analysis, cells were washed once in PBS and fixed with 70% ethanol at -20°C for 30 minutes. Cells were then washed and resuspended in PBS-0.1% Triton complemented with 100 µg/mL RNAse A (Sigma) and 5 µg/mL propidium iodide (BD, 51-66211E) at 37°C for 30 minutes. After PBS washing, cellular DNA contents were assayed by flow cytometry.

Target	*Fluorochrome*	*Manufacturer*	*Reference*
CD3	FITC	Miltenyi	130-113-138
	VioBlue	Miltenyi	130-110-460
CD56	APC-Vio770	Miltenyi	130-114-548
	FITC	Miltenyi	130-100-683
CD69	PE	Miltenyi	130-112-651
CD14	APC-Vio770	Miltenyi	130-110-552
	PE	Miltenyi	130-110-519
CD45	FITC	Miltenyi	130-110-633
	APC	Miltenyi	130-113-114
CD15	PE-Vio770	Miltenyi	130-113-486
IFNa	PE	Miltenyi	130-116-873
ICAM-1	APC	Miltenyi	130-121-342
MICA/B	PE	Miltenyi	130-118-829
Annexin-V	FITC	Miltenyi	130-093-060
7AAD	-	ThermoFisher	00-6993-50

Supplementary Table 1: Antibodies used for Flow Cytometry

In vivo Bioluminescence Imaging

The engraftment of AML bioluminescent cell lines (THP-1-LucZsGreen and U937-LucZsGreen) was assessed by bioluminescence imaging using an IVIS Spectrum In Vivo Imaging System (Perkin Elmer). Mice were intraperitoneally injected with 3 mg of D-luciferin resuspended in 0.9% NaCl, 20 min before imaging and were then anesthetized using 2.5% Isoflurane. Mean of total body bioluminescent signal quantification (photons/ROI/min) of regions of interest was carried out using Living Image software.

In vivo treatments

Once engrafted, mice were assigned to the different treatment arms based on tumor burden and body weight. AZA (2 mg/kg) was administered by intra-peritoneal injection, TAK-981 (15 mg/kg) by caudal tail vein injection and venetoclax (50 mg/kg) by oral gavage. Immediately before administration, AZA was solubilized in 0.9% NaCl, TAK-981 in 20% HPBCD (hydroxypropyl beta-cyclodextrin) and venetoclax in corn oil (SIGMA, C8267) with 30% PEG400 and 10% ethanol. Evolutions of tumor burden were monitored by bioluminescence (cell lines) or by flow cytometry (hCD45+ cells) in the peripheral blood (primary AML cells). Mice were monitored daily for symptoms of distress defined by the Ethical Committee (ruffled coat, hunched back, and reduced mobility) to decide the time of killing of injected animals.

Analysis of SUMOylation activity in bone marrow cells

Bone marrows (from tibias and femurs) were flushed and cells were rinsed in PBS. After red blood cells lysis using the ACK lysis buffer (A1049201, Gibco), mononuclear cells from bone marrow were counted and equal number of cells were used to prepare extracts and monitor SUMOylation activity as previously described[2]. Briefly, 2.10^6 cells are resuspended in 50 µL of swelling buffer (20 mM Hepes pH 7.5, 1.5 mM MgCl2, 5 mM KCl, 1mM DTT, 1 µg/mL aprotinin, pepstatin, leupeptin), incubated on ice vortexing every 5 min for 30 min, lysed with 4 freeze/thaw cycles and passed through an hamilton seringe to shear DNA. After centrifugation, extracts are supplemented with 0.5µM SUMO-vinyl sulfones (Boston Biochem) and mixed and incubated for 45 min at 30 °C with XMap Luminex beads coupled to the ZMYM-5 protein, 2 mM ATP, 10 µM SUMO-1 in 20 mM Hepes pH 7.3, 110 mM KOAc, 2 mM Mg(OAc)2, 0.05% Tween-20, 0.5 mM EGTA, 0.2 mg/mL ovalbumin, 1 mM DTT, 1 µg/mL aprotinin, pepstatin, leupeptin. After washes with PBS, 0.05% Tween-20, 0.5% SDS, beads are incubated with mouse anti-SUMO-1 antibody (21C7) for 1 hr, washed with PBS, 0.05% Tween-20 and

incubated with Alexa-Fluor 488-coupled secondary antibody for 30 min before analysis by flow cytometry[2].

RNA-seq libraries preparation and sequencing

Total RNAs were purified using the GenElute Mammalian Total RNA kit (Sigma-Aldrich), treated with DNase I (New England Biolabs) and re-purified. RNA quality was assessed using a BioAnalyzer Nano 6000 chip (Agilent). Three independent experiments were performed. Libraries were prepared using TruSeq®Stranded mRNA Sample Preparation kit (Illumina). After the PCR amplification step, PCR products were purified using AMPure XP beads (Agencourt Biosciences Corporation). The quality, size and concentration of cDNA libraries were checked using the Standard Sensitivity NGS kit Fragment Analyzer and qPCR (ROCHE Light Cycler 480). Libraries were sequenced using an Illumina Novaseq 6000 sequencer as paired-end 150 base reads. Replicates 1 and 2 were sequenced on the Montpellier Genomix facility (MGX) and replicate 3 on the CNAG platform (Center for Genomic Regulation, Barcelona, Spain). Image analysis and base calling were performed using the NovaSeq Control Software, Real-Time Analysis 3 (RTA) and bcl2fastq. The RNA-Seq sequencing data are available on Gene Expression Omnibus with accession number GSE212330 (token for reviewers: wzcveigafrkhrob)

RNA-seq mapping, quantification and differential analysis

RNA-seq reads were mapped on the Human reference genome (hg38, GRCh38p12) using TopHat2 (2.1.1)[3] based on the Bowtie2 (2.3.5.1) aligner[4]. Reads association with annotated gene regions was done using the HTseq-count tool v0.11.1[5]. Differential expression analysis was performed with DESeq2[6] using normalization by sequencing depth and parametric negative binomial law to estimate the data dispersion. Genes with a fold change ≥ 2 or ≤ 0.5 and an adjusted p-value < 0.05 were considered differentially expressed. Gene Set Enrichment Analyses were performed using https://www.gsea-msigdb.org/gsea/index.jsp (version 4.0.3)[7].

RT-qPCR assays

After DNase I treatment, 1 µg of total RNA purified as described above was used for cDNA synthesis using the Maxima First Strand cDNA kit (ThermoFisher Scientific). qPCR assays were conducted using Taq platinum (Invitrogen) and the LightCycler 480 device (Roche) with specific DNA primers (IDT, sequence available on request). Data were normalized to the mRNA levels of the *GAPDH* housekeeping gene.

Supplementary references

1 Yadav B, Wennerberg K, Aittokallio T, Tang J. Searching for Drug Synergy in Complex Dose–Response Landscapes Using an Interaction Potency Model. *Comput Struct Biotechnol J* 2015; **13**: 504–513.

2 Recasens-Zorzo C, Gâtel P, Brockly F, Bossis G. A Microbead-Based Flow Cytometry Assay to Assess the Activity of Ubiquitin and Ubiquitin-Like Conjugating Enzymes. *Methods Mol Biol Clifton NJ* 2023; **2602**: 65–79.

3 Kim D, Pertea G, Trapnell C, Pimentel H, Kelley R, Salzberg SL. TopHat2: accurate alignment of transcriptomes in the presence of insertions, deletions and gene fusions. *Genome Biol* 2013; **14**: R36.

4 Langmead B, Salzberg SL. Fast gapped-read alignment with Bowtie 2. *Nat Methods* 2012; **9**: 357–359.

5 Anders S, Pyl PT, Huber W. HTSeq—a Python framework to work with high-throughput sequencing data. *Bioinformatics* 2015; **31**: 166–169.

6 Love MI, Huber W, Anders S. Moderated estimation of fold change and dispersion for RNA-seq data with DESeq2. *Genome Biol* 2014; **15**. doi:10.1186/s13059-014-0550-8.

7 Subramanian A, Tamayo P, Mootha VK, Mukherjee S, Ebert BL, Gillette MA *et al.* Gene set enrichment analysis: A knowledge-based approach for interpreting genome-wide expression profiles. *Proc Natl Acad Sci* 2005; **102**: 15545–15550.

Supplementary Figures and Tables

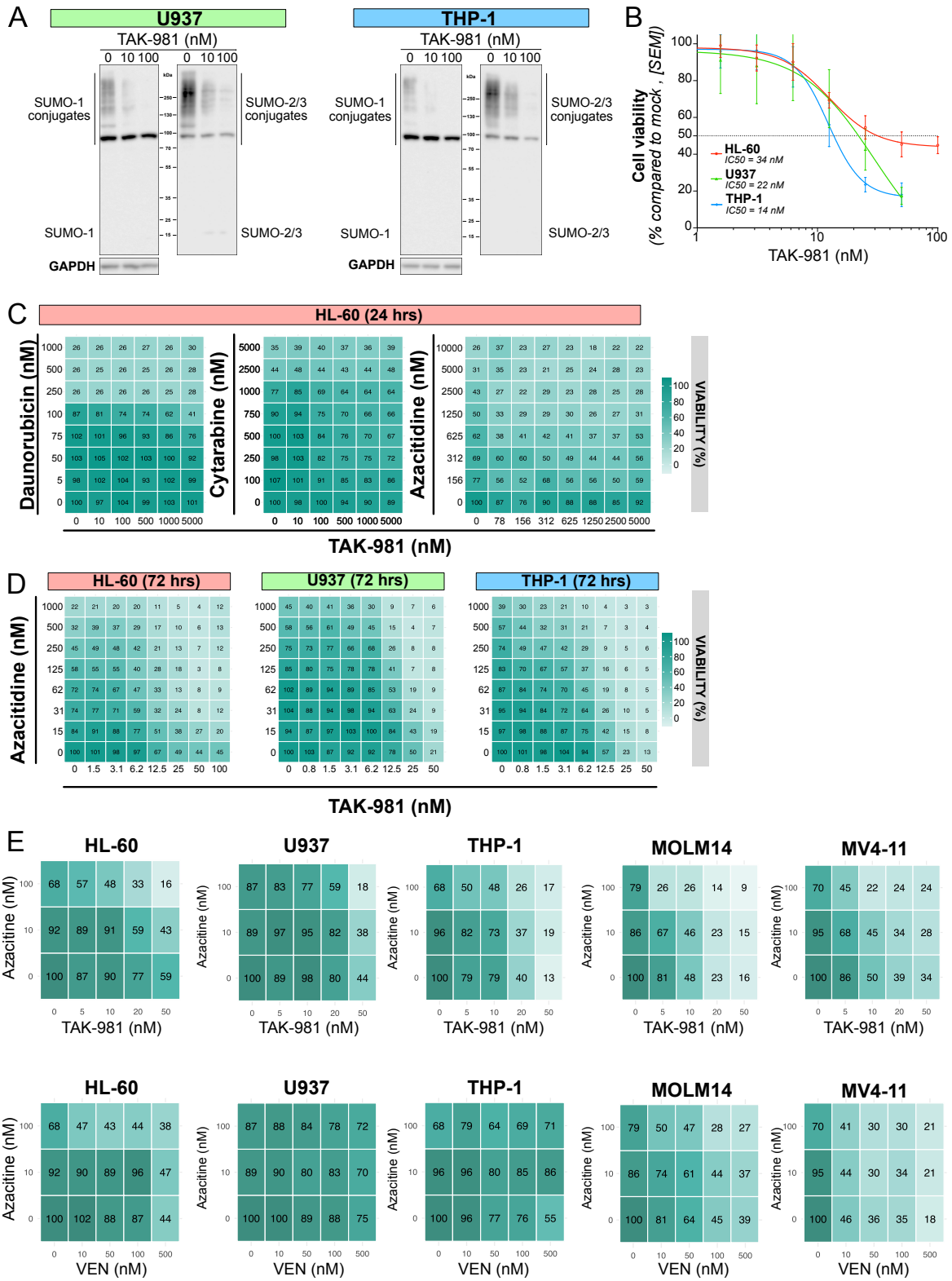

Supplementary Figure 1: TAK-981 induces deSUMOylation and synergize with Azacitidine to induce death of AML cell lines

A) U937 and THP-1 cells were treated with 10 nM or 100 nM of TAK-981 for 24 hours and immunoblots were performed for SUMO-1, SUMO-2/3 and GAPDH. **B)** IC_{50} determination of

HL-60, U937 and THP-1 cell lines treated with TAK-981 at concentrations ranging from 1 to 100 nM for 72 consecutive hours. Cell viability was determined by MTS assays 24 hours after the last addition of drug and compared to that in mock-treated conditions. Concentration-response curves were generated comparing the viability in TAK-981 treated conditions with mock-treated controls (n=3, mean +/- SEM, absolute half-maximal inhibitory concentrations (IC_{50}) are shown). **C)** Heat maps showing the median percentage of viability of HL-60 cells treated for 24 hours with TAK-981 and either DNR, ARA-C or AZA compared to mock-treated conditions, assessed by MTS assay (median of 3 independent experiments for each drug). **D)** Heat maps showing median percentage of viability for HL-60, U937 and THP-1 cells treated with TAK-981 and AZA every day for 3 consecutive days. Viability was analyzed at day 4 by MTS and compared to that in mock-treated conditions (median of 3 independent experiments for each cell line). **E)** Heat maps showing median percentage of viability for HL-60, U937, THP-1, MOLM14 and MV4-11 cells treated with AZA (10 or 100 nM) combined to TAK-981 (5, 10, 20, 50 nM) or VEN (10, 50, 100, 500 nM) every day for 3 consecutive days. Cell viability was determined by MTS assays 24 hours after the last addition of drug and compared to that in mock-treated conditions (median of at least 3 independent experiments for each cell line).

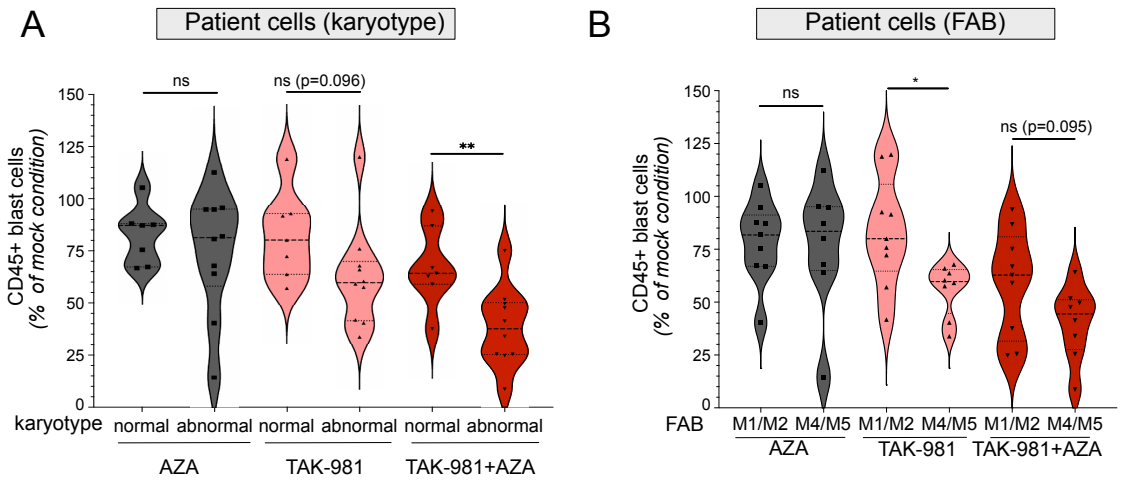

Supplementary Figure 2. Patient cells with abnormal karyotypes and from the M4/M5 FAB subtypes are more sensitive to TAK-981+AZA. Patient (n = 17) bone marrow mononuclear cells were treated for 3 consecutive days (Day 1, 2, 3) with TAK-981 (10 nM) and/or AZA (100 nM) and kept in culture. After 8 days, cells were collected and the number of CD45+ cells was analyzed by flow cytometry in each condition and compared to the mock-treated condition. For each group, plain lines represent the median value, and dotted lines are the quartiles. Groups were compared using unpaired t-test after sorting the patients depending on their karyotype (normal or abnormal)(A) or FAB subtype (M1/M2 or M4/M5).

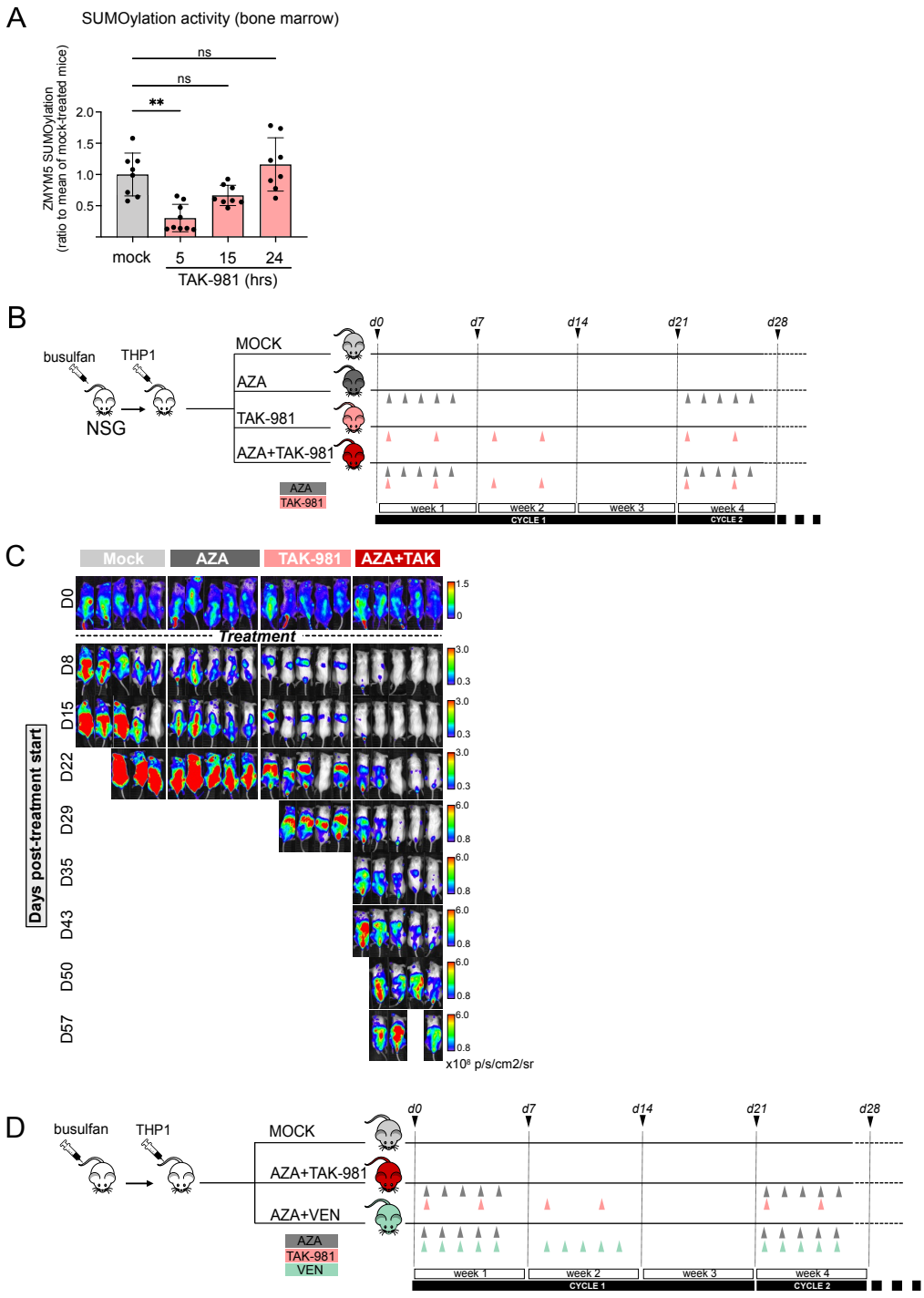

Supplementary Figure 3: TAK-981 and AZA combination has a higher anti-leukemic activity than monotherapies *in vivo.* A) NSG mouse (8-9 mice/group) were treated with TAK-981 (15 mg/kg) for the indicated times. Extracts from bone marrow cells were used in microbeads-based assay to monitor the activity of SUMOylation enzymes. **B)** NSG mouse treatment schedule for experiments conducted in Figure 2A and 2B. **C)** Quantification, as photons/second/cm^2/sr of tumor burden evolution monitored by luminescence intensity in mice (5/group) injected with bioluminescent THP-1 cells. **D)** Schematic representation of mouse treatment schedule for experiments conducted in Figure 2C and 2D.

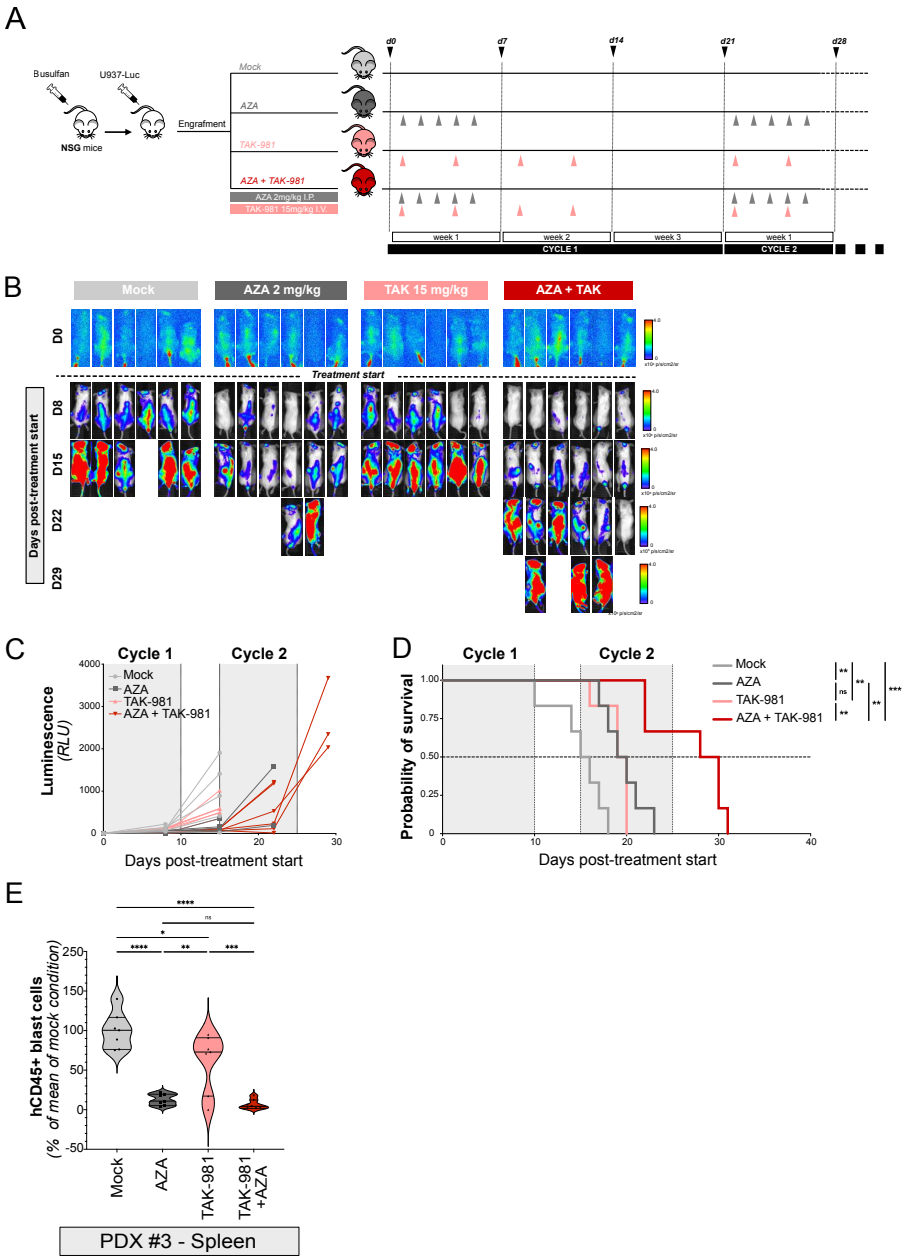

Supplementary Figure 4: TAK-981 and AZA combination has higher anti-leukemic activity than monotherapies on U937 cells *in vivo*. A) NSG mice treatment schedule for experiments conducted in B, C and D. **B-C)** Quantification as photons/second/cm2/sr (B) and relative luminescence units (C) of tumor burden evolution monitored by luminescence intensity in mice (6/group) injected with bioluminescent U937 cell line. **D)** Overall survival after treatment start of mice injected with bioluminescent U937 cell line was estimated in each group and compared with Kaplan-Meier method and log-rank test. **E)** NSG mice were injected with primary cells from one AML patient (PDX#3). After engraftment, mice were treated with AZA and/or TAK-981 and euthanized at day 9. The total number of human CD45+ cells (hCD45) was estimated by flow cytometry in spleen and compared to the mean number of cells collected in the mock-treated group of mice. For each group, plain lines represent the median value, and dotted lines are the quartiles. Groups were compared using Ordinary one-way ANOVA test.

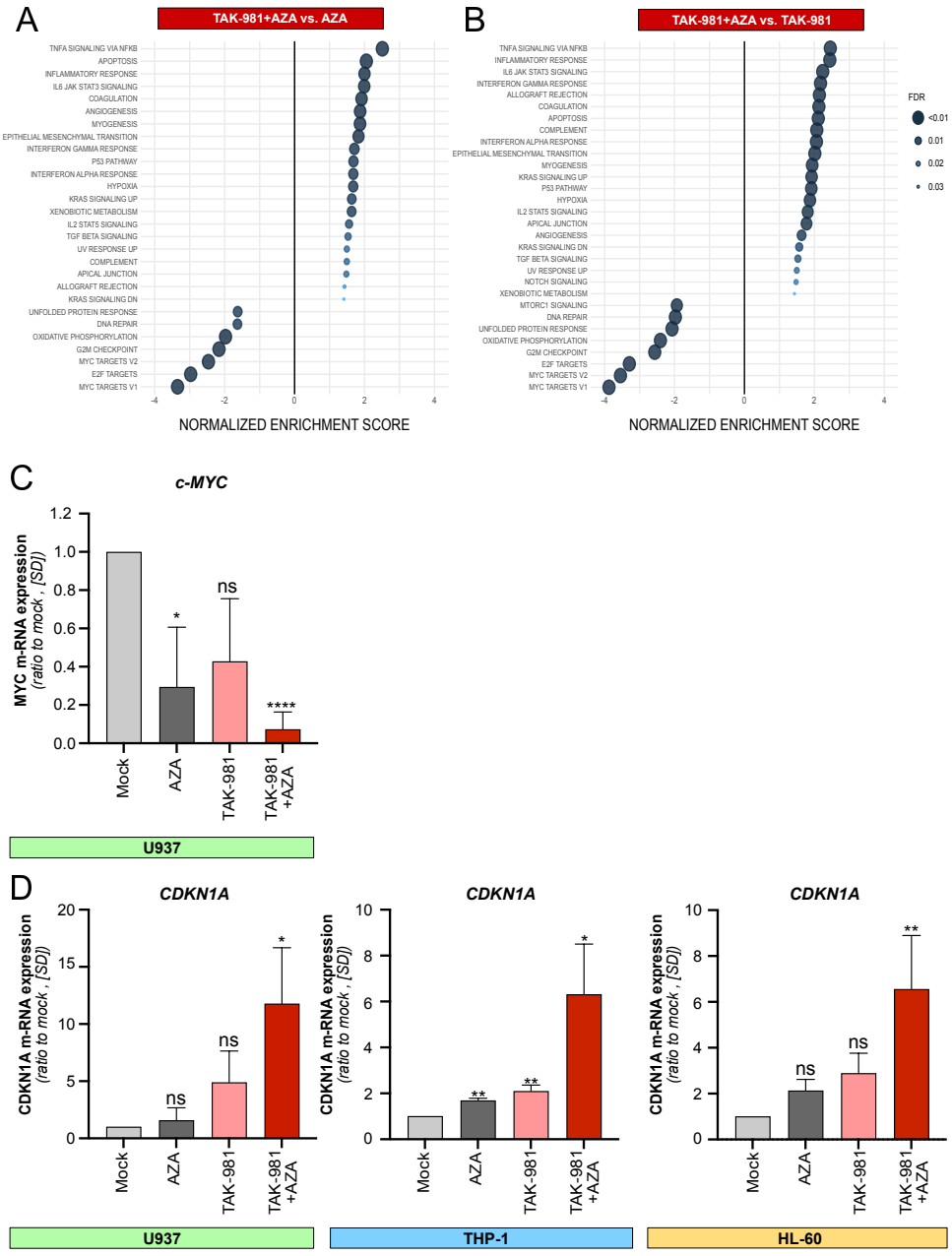

Supplementary Figure 5: Gene expression signatures in U937 cells treated with TAK-981 and AZA

A, B) GSEA were performed using Hallmark datasets on the RNA-Seq data obtained from U937 cells. All pathways significantly enriched upon TAK-981+AZA compared to AZA (A) or TAK-981 (B) are shown (abs(NES)>1, p<0.05 and FDR<0.05). C) mRNA expression of *c-MYC* was analyzed by qRT-PCR in U937 cells treated for 72 hours with 10 nM AZA and 10 nM TAK-981. Results were normalized to *GAPDH* mRNA levels and expressed as ratio to mock-treated cells (n=5, mean +/- SD, one-way ANOVA). D) mRNA expression of *CDKN1a* was analyzed by qRT-PCR in U937 cells treated for 72 hours with 10 nM AZA and 10 nM TAK-981, THP-1 and HL-60 treated with 100 nM AZA and 10 nM TAK-981 (n=5 for U937, n=4 for THP1, n=3 for HL-60, mean +/- SD, one-way ANOVA)

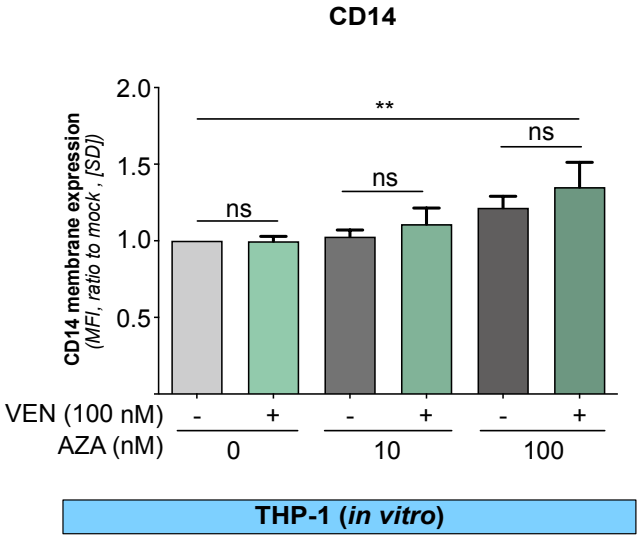

Supplementary Figure 6: Effect of VEN+AZA on THP1 differentiation. Membrane expression of CD14 was measured by flow cytometry on THP-1 treated with AZA (10 or 100 nM) and 100 nM VEN or the drug combination for 72 hours. MFI were normalized to that of mock-treated cells (n=3, mean +/- SD, One-way ANOVA test)

Supplementary Tables (see excel files)

Supplementary Table 2: Clinical characteristics of the patient samples used in this study.

Supplementary Table 3: Raw data for the RNA-Seq analysis of U937 cells treated with TAK-981, AZA or TAK-981+AZA. The comparison between each experimental condition (3 biological replicates) is provided as Fold Changes and associated p-values.

Supplementary Table 4: Gene Set Enrichment Analysis of the U937 RNA-Seq data. GSEA analysis were performed on the Hallmarks and Gene Ontology Biological Process. For each gene signature, Enrichment Scores (ES) and Normalized Enrichment Scores (NES) as well as the associated p-values and False Discovery Rates (FDR) are provided for TAK-981-, AZA- or TAK-981+AZA versus mock-, AZA- and TAK-981-treated cells.